

TAT

C6

no. 62-73

C. E. - R. R. COPY

COPY 2

A FLOW MEASURING DEVICE DEPENDING ON THE DRAG
DEVELOPED ON A WIRE SUSPENDED IN WATER

By

Bruce B. Sharp

Colorado State University
Civil Engineering Department
in association with
U. S. Department of Agriculture
Agricultural Research Service

ENGINEERING RESEARCH
JUN 21 '73
FOOTHILLS READING ROOM

December 1962

CER62BBS73

A FLOW MEASURING DEVICE DEPENDING ON THE DRAG
DEVELOPED ON A WIRE SUSPENDED IN WATER

By

Bruce B. Sharp

Colorado State University
Civil Engineering Department
in association with
U. S. Department of Agriculture
Agricultural Research Service

December 1962

CER62BBS73



U18401 0593974

CONTENTS

I	INTRODUCTION	1
II	CONSTRUCTION FEATURES	1
	A. Conduit Installation	1
	B. Probe Instrumentation	3
III	GENERAL ANALYSIS	5
	A. Equilibrium Conditions	5
	B. Drag Integral	6
	C. Generalized Interpretation of Test Results	6
	D. Further Discussion of the Drag Integral	8
	E. The Influence of the Wire Characteristics	9
IV	TEST RESULTS	10
	A. Conduit Studies	10
	B. Suspension Wire Probe	31
V	SUSPENSION WIRE PROBE - DYNAMIC RESPONSE	35
VI	SUSPENSION WIRE PROBE - RESPONSE TO SEDIMENT LOAD	35
VII	RECOMMENDATIONS	37
	ACKNOWLEDGEMENTS	39
	REFERENCES	39

FIGURES

Figure		Page
1	Suspension wire conduit installation	2
2	Suspension wire installation	2
3	Wiring diagram	3
4	Suspension wire probe	4
5	Suspension wire - definition sketch	5
6	Velocity profile for axisymmetric flow	6
7	Generalized interpretation of test results	7
8	Velocity distribution - 2.06" dia. conduit	11
9	W4 (Brass conduit)	14
10	W3 (Brass conduit)	15
11	W5 (Brass conduit)	16
12	Velocity distribution - 2.04" dia. conduit	17
13	W7 (Plastic conduit)	18
14	W1 (Plastic conduit)	19
15	W6 (Plastic conduit)	20
16	W5 (Plastic conduit)	21
17	Correlation of test results with R_w	22
18	Velocity distribution water tunnel	23
19	W1 (Water tunnel)	24
20	W5 (Water tunnel)	25
21	W6 (Water tunnel)	26
22	Water tunnel tests	27
23	Drag on fixed cylinders, infinite length (Wieselsberger)	29
24	Influence of wire characteristics	30
25	Suspension wire probe	32
26	Flume test-suspension wire probe	33
27	Suspension wire probe - 8 in. wide flume	34
28	Suspension wire probe - dynamic response	36
29	Suspension wire probe - response to sediment load (8" x 8" tilting flume)	38

TABLES

Table		Page
I	Wire data	10
II	2.06" dia. brass conduit $F_v = 1.07$	12
III	2.04" dia. plastic conduit $F_v = 1.01$	12&13
IV	12" x 6" water tunnel $F_v = 1.00$	28&30
V	Results of flume test - suspension wire probe drag measurements	31
VI	Suspension wire probe - dynamic response	35

A FLOW MEASURING DEVICE DEPENDING ON THE DRAG
DEVELOPED ON A WIRE SUSPENDED IN WATER

I. INTRODUCTION

The displacement characteristics of a thin wire suspended in a closed conduit and an open channel have been studied. Results of a qualitative nature only, have been sought, sufficient to demonstrate the operating principle of an instrument that has been developed for relative velocity and drag measurements.

An investigation of the drag on a wire in a closed conduit was initiated at the University of Melbourne in 1961, where the writer assisted by C. E. Kirkham (then engaged in research as a Commonwealth Fellow), studied several types of wire in a 5.2" diameter clear plastic water pipe flowing full. The meager results at that time suggested that a systematic study would be worthwhile and assistance to do this has been provided by the Civil Engineering Department of Colorado State

University in association with the Agricultural Research Service.

The suspension wire derives its operating principle from that of a catenary and wires varying in diameter from 0.001 to 0.0071 inches have been subjected to the drag of the water in 2" nominal diameter conduits and a 11" x 5-1/2" working section water tunnel. Also a 'suspension wire' probe has been built and the drag in a rectangular water channel has been observed including measurements within a wire diameter of the floor of the channel.

A small study of the vortex street frequency from cylinders has been performed to test the response characteristics of the device, and the behavior of the suspension wire probe in channel water flow with a heavy sediment load has been investigated.

II. CONSTRUCTION FEATURES

A. Conduit Installation

The wire was suspended across the flow with one end clamped while the other was elastically supported. The elastic support provided both a restoring force and a means for measuring the displacement of this end.

Figure 1 shows the structural features of the lower clamped end support. Also shown is the small box which houses the beam or elastic support on which was mounted a semi-conductor strain gauge as the active arm of a Wheatstone Bridge circuit. A dummy gauge was also placed in the box to provide temperature compensation.

A typical installation is illustrated in the plate in Fig. 2. In this instance the conduit consisted of a smooth brass pipe with a measuring station for the determination of velocity distribution at the downstream end, (flow, left to right in the figure).

The immediate problem of keeping the wire clean was accomplished with a metal shield. The shield, consisting of brass tube 0.125" external diameter was designed to traverse the conduit and cover the wire, without interfering with the clamped lower support. The wire was exposed only for the length of time necessary to take a reading.

The shield accomplished two additional requirements, namely temperature and pressure compensation with respect to the wire itself.

Temperature compensation is necessary when it is realized that very small movements are measured and differential expansion or contraction of the conduit and the wire is possible, producing a strain on the beam. The shield does not prevent the wire and the conduit from reaching an equilibrium state and differential movement may be rendered insignificant, even if it occurs, by the short duration of actual measurements.

Pressure compensation is similarly achieved and it was apparent during the tests that inadequate external support of the box (which should be rigidly attached to the conduit) would lead to more serious errors than temperature effects. An external clamp for the box can be seen in Fig. 2.

The clamped lower end was positioned to correspond with the interior face of the wall of the conduit. It proved convenient in determining the basic operating principle of the instrument to move the clamp to adjust the initial tension on the wire and consequently the effective length of the wire varied by a small amount.

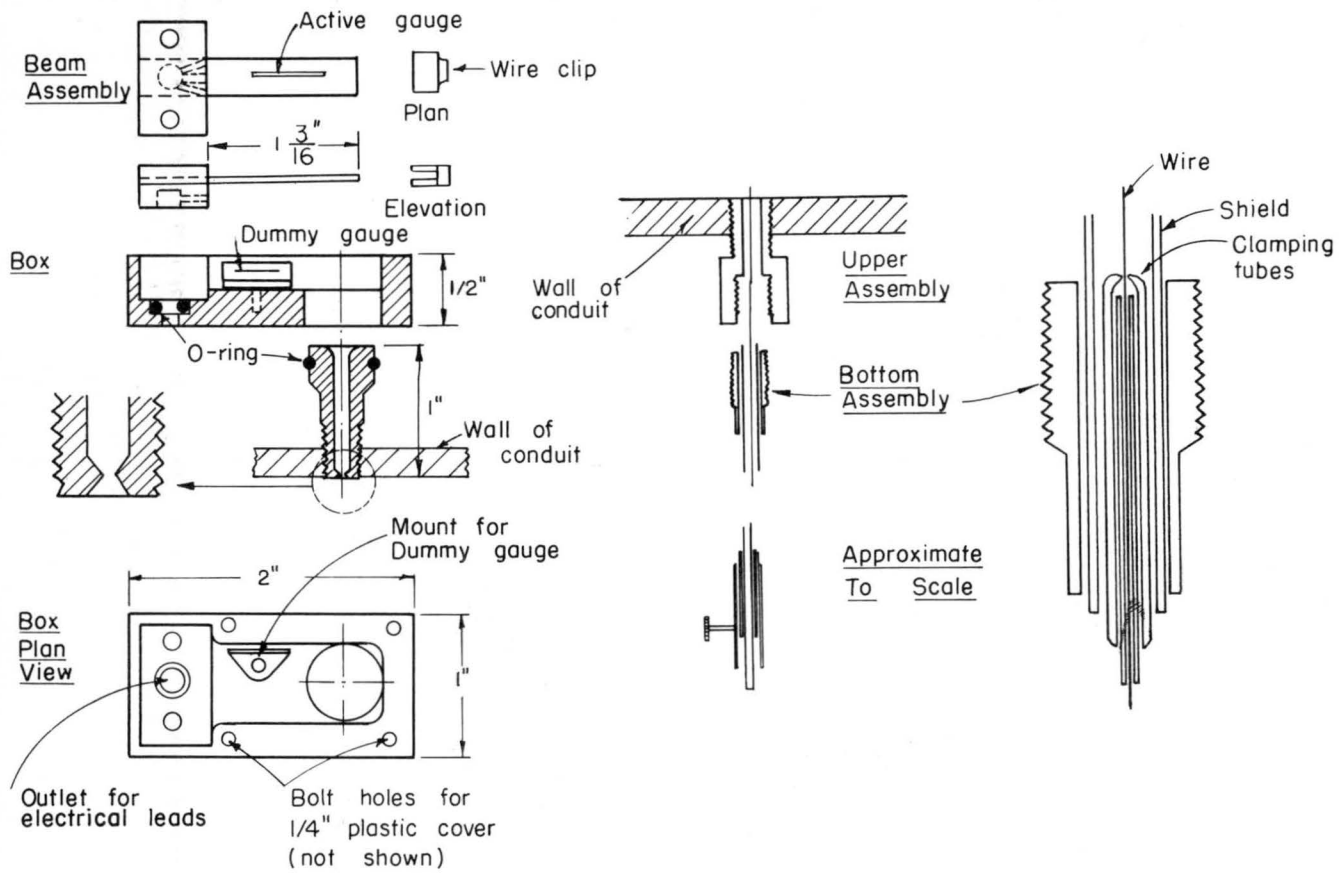


FIG. 1 SUSPENSION WIRE CONDUIT INSTALLATION

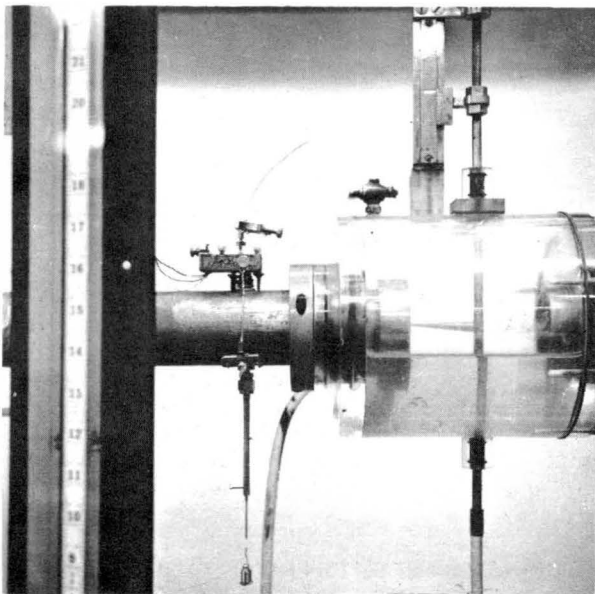


FIG. 2 SUSPENSION WIRE INSTALLATION

Calibration of the elastic support and the attendant electronic equipment was readily effected at any time by weights attached to the wire which could be unclamped and hung freely, vertically.

It should be apparent that the design of the lower support in these preliminary investigations was a crucial problem and the method illustrated allows the device to be returned to zero drag at any instant irrespective of the conditions in the conduit. This unique feature overcomes a number of seemingly obvious disadvantages that appear at first sight and in ultimate developments this facility might be discarded with some reluctance.

When studies were being made in the 11" water tunnel, a similar design of lower support was used successfully.

The upper elastic support consisted of a beam of phosphor bronze of one inch effective length. A semiconductor strain gauge of type MS 132-350 and manufactured by Micro Systems Incorporated was mounted in a convenient position to be in tension. It was assumed that the deflection of the beam at the point where the wire was attached would be linearly related

to the strain on the gauge. The active and dummy gauges were both waterproofed according to the manufacturer's directions with epoxy resin, as the interior of the box was filled with the operating fluid.

In a later installation the ambient and water temperatures differed to a greater extent and some difficulty was experienced in obtaining rapid temperature compensation mainly because of the box design.

The indicating equipment consisted of a simple Wheatstone Bridge in which a direct current supply was derived from one or several Mallory type Mercury cells each having an output of 1.35 volts; see Fig. 3. The bridge output was observed directly by a Leeds Northrup Precision Galvanometer without the use of a preamplifier. The sensitivity of the galvanometer was 0.0035 microamps per centimeter deflection.

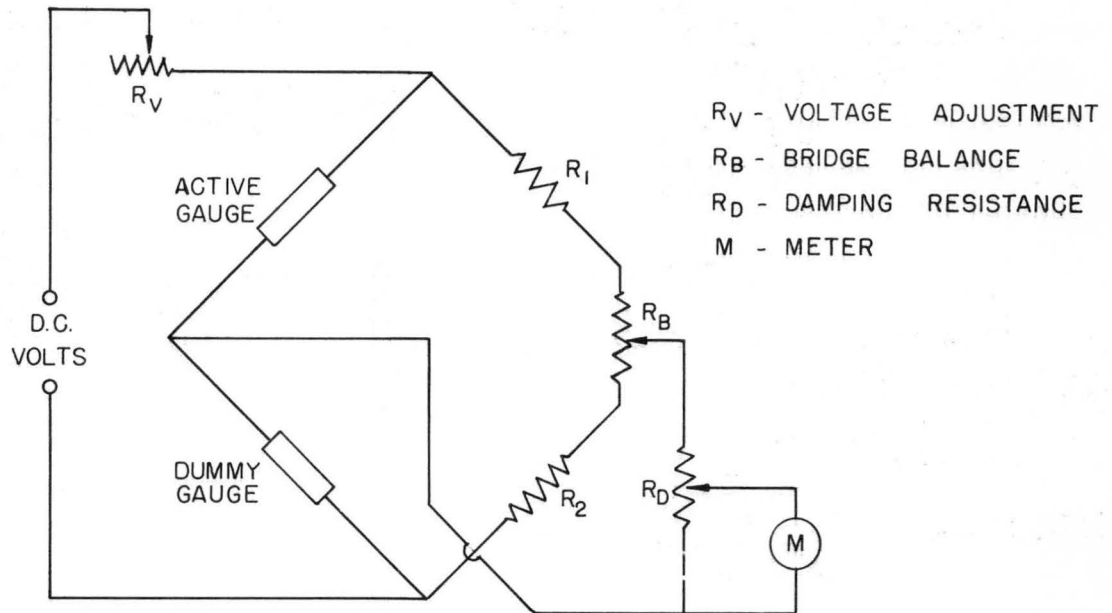


FIG. 3 WIRING DIAGRAM

B. Probe Instrumentation

The features described in A were retained as fully as possible in the design of the probe with the exception of the shield as shown in Fig. 4.

In this case, to zero the instrument the probe was rotated so that the wire became parallel to the flow of the water. This elimination of the drag effects may not be complete and in certain circumstances special precautions would need to be taken.

The clamped end in this instance was such that adjustment of the wire tension could not be readily achieved in the flow. If this should be necessary, a spreader which would strain the fork of the probe is considered the best approach. The fork of the probe was played slightly in manufacture, and this was

considered a possible advantage in reducing the edge effects of the fork extensions.

The beam, now 1/8" wide, was checked initially for clearances by first covering the beam with a transparent plastic tube. Both arms of the fork were then eventually fitted with slipon bull-nose brass covers that readily allow renewal and adjustment of the wire. In the arm with the fixed support a dummy gauge was mounted on a strip of phosphor bronze similar to the beam and achieved the necessary temperature compensation.

Calibration was performed by weights attached to the wire and the probe rotated with the wire vertical. The trailing end of the wire beyond the clamp was left intact and did not interfere with flow conditions in the use of the probe.

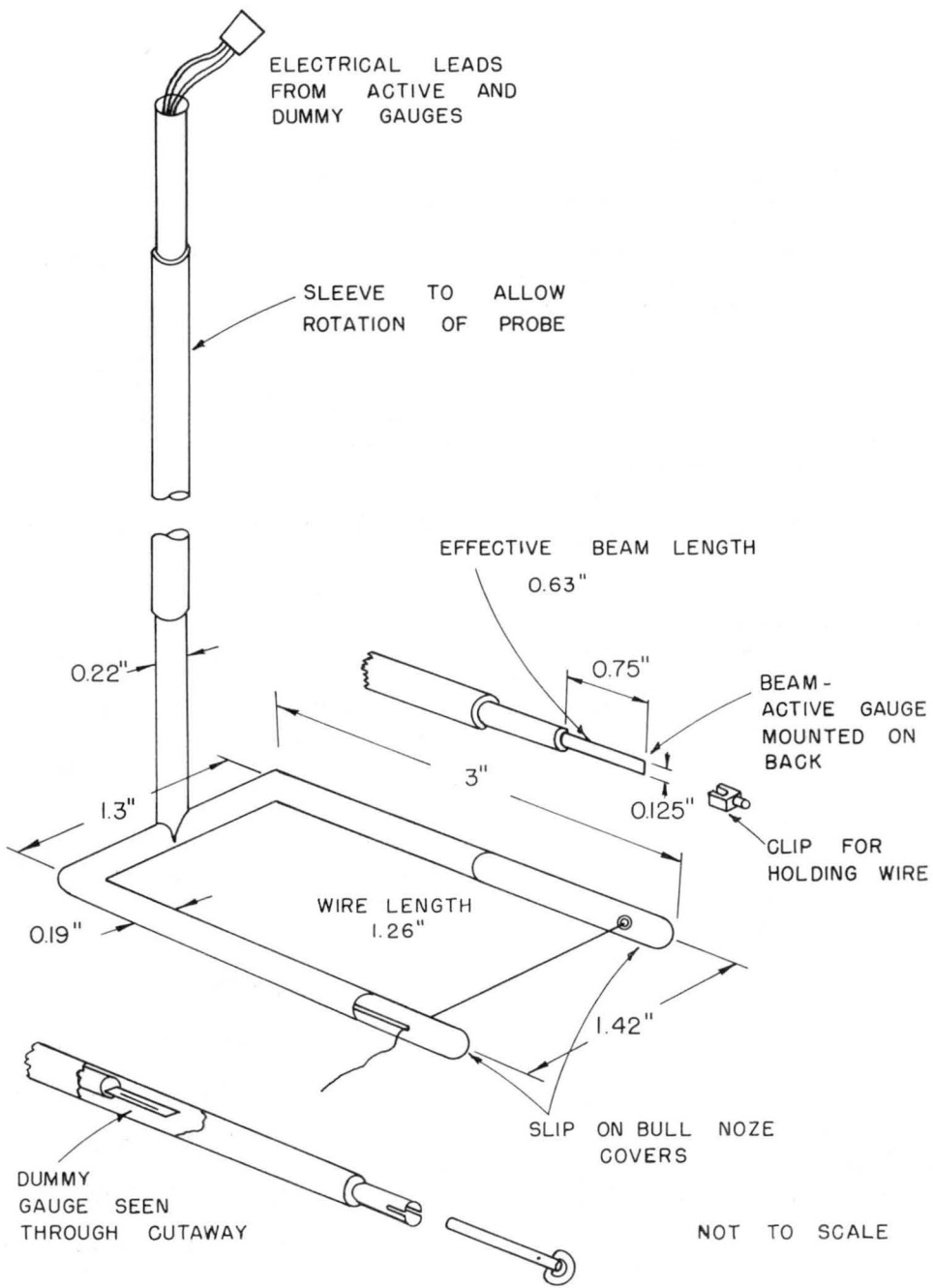


FIG. 4 SUSPENSION WIRE PROBE

The electronic equipment was the same previously described except for the observations of the turbulent wake from a cylinder. In this case a pre-amplifier with a gain of 100 or 1000 was used to

amplify the bridge output for examination on a cathode ray oscilloscope. An audio oscillator input to the normal sweep axis completed the equipment necessary for studying the Lissajou figures produced.

III. GENERAL ANALYSIS

The suspension wire is subjected to drag forces due to the flow of water. There is considerable literature available on the drag on a cylinder, largely rationalizing the problem in the case of fixed cylinders. For example, recently A. Roshko (1961) summarized the results of drag coefficients and the value of the Strouhal number up to a Reynolds number of 10^6 , stressing various critical regions.

The nature of the drag on a wire completely traversing a conduit, however, is an extremely complex one, involving not only a variable velocity distribution but also an unknown factor due to the self induced oscillations of the wire. This latter effect of course is associated with the vortex street generated by the wire, and some observations on this aspect have been made by D. B. Steinman (1946) and H. Rouse (1956).

The analytical discussion attempts to describe the equilibrium conditions for the wire under the action of a non-uniform load. The experimental procedures endeavored to test the basic assumptions while to a limited extent the physical characteristics of the wire were also investigated.

In addition the relationships between the load measurement, the integration of the drag effects and the velocity of the fluid have been studied in order to define the quantity that was being observed.

A. Equilibrium Conditions

A wire supporting only its own uniform self-weight and unable to sustain any lateral bending is referred to as a catenary. A wire which differs mainly in carrying a non-uniform load that might render its self weight insignificant requires but an extension of the catenary principle.

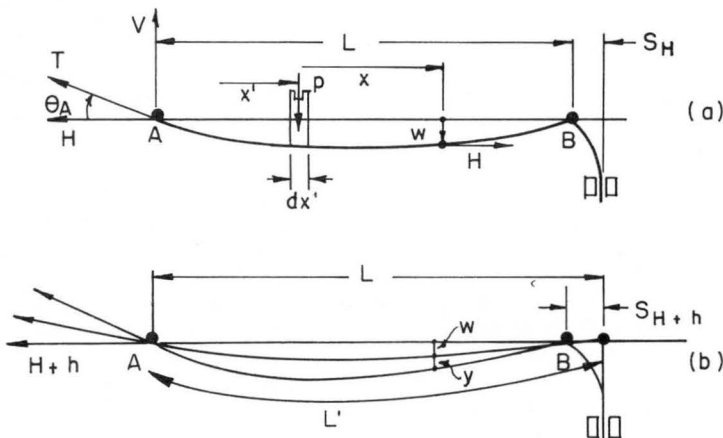
Referring to the definition sketch in Fig. 5(a) and in a manner demonstrated by T. von Karman and M. A. Biot (1940), equilibrium equations may be expressed as follows.

$$-Hw + Hx \tan \theta_A + \int_0^x (x' - x) p(x') dx' = 0 \quad (1)$$

$$\text{and} \quad H = k_1 S_H \quad (2)$$

Equation (1) is essentially a moment equation, in which the individual terms in order represent, the moment of the horizontal component of the wire tension, the moment of the fixed end vertical reaction and the moment of the non-uniform distributed load to the left of the point (x, w) .

Equation (2) expresses the quantity to be measured in terms of the deflection of the elastic of the beam support.



Symbols

- L , Wire span. L' , Total wire length
- p , Portion of distributed load at x'
- H & V , Components of wire tension T
- w, y , Wire deflections at x
- w_c , Wire deflection at $L'/2$
- S , Deflection of beam
- θ , Slope of wire

FIG. 5 SUSPENSION WIRE - DEFINITION SKETCH

The physical characteristics of the wire in particular demand a more general expression of the equilibrium conditions involving the additional terms shown in Fig. 5(b), and leading to a modification of the above equations to the forms shown below.

$$-(H+h)(w+y) + (H+h)x \tan \theta_A + \int_0^x (x'-x) p(x') dx' = 0 \quad (3)$$

$$(H+h) = k_1 S_{H+h} \quad (4)$$

Equation (3) extended to apply to the whole wire then becomes:

$$(H+h) L \tan \theta_A = - \int_0^L (x'-L) p(x') dx' \quad (5)$$

In all tests the elongation of the wire appeared to have a very important bearing in the interpretation of the results and for this reason the tests were designed to study the effect of variation of the initial wire tension on the drag reading for a constant flow (and hence constant drag).

If it is considered that the wire suffers only small displacements, then a suitable approximation of the wire shape is a parabola. With this assumption the following relations may be derived (refer to Fig. 5).

$$\tan \theta_A = k_2 \frac{w}{L} \quad (6)$$

$$(L'-L) L = k_3 w_c^2 \quad (7)$$

The incremental variation of the quantities can then be expressed as

$$d(\tan \theta_A) = d\left(\frac{w}{L}\right) = -k_4 dL = k_5 dS \quad (8)$$

The last equation shows that it is permissible to assume that the variation of $\tan \theta_A$ is linearly related to the variation of the beam deflection or, to a shift of the 'fixed' end of the wire.

Equation (5) may then be approximated by:

$$\text{constant } (H+h) \cdot (h) = - \frac{1}{L} \int_0^L (x'-L) p(x') dx' \quad (9)$$

If now the right-hand side of Equation (9) is constant, the effect of varying the initial tension of the wire can be investigated. This requires some further interpretation of the 'drag integral' on the right-hand side of Equation (9).

B. Drag Integral

The relationship of the 'line integration' performed by the wire to flow conditions will be discussed later, for the moment it is desired to show that by a suitable shift of origin the integral may be modified and a specific case considered.

In Fig. 6 is illustrated a velocity distribution for axisymmetric flow. The drag integral may be written in the expanded form:

$$\int_{-\frac{L}{2}}^{+\frac{L}{2}} f(u) \cdot (r - \frac{L}{2}) dr = -\frac{L}{2} \int_{-\frac{L}{2}}^{+\frac{L}{2}} f(u) dr + \int_{-\frac{L}{2}}^{+\frac{L}{2}} f(u)r dr \quad (10)$$

where $f(u)$ represents an unknown relationship between the drag on the wire and the stream velocity at a point r from the axis of symmetry. In this case of symmetry the last integral on the right-hand side of Equation (10) is zero and thus the wire line integration is of the form,

$$I_w = \int f(u) dr$$

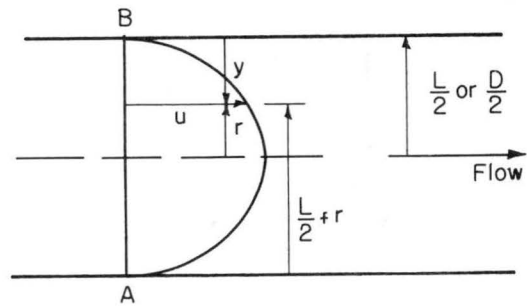


FIG. 6 VELOCITY PROFILE FOR AXISYMMETRIC FLOW

The physical explanation for this transformation is evident in reference to Equation (5) which shows that the drag integral must be the integrated moment of the load about a support and for a symmetrical load this may be replaced by the moment of the total load effectively acting at the center of the span.

Equation (9) then becomes, for the purpose of studying the effect of varying the initial wire tension,

$$(H+h) h = \text{constant} \quad (11)$$

C. Generalized Interpretation of Test Results

Readings of drag, represented by h , and readings of initial tension plus drag, represented by $H+h$, have been plotted on loglog paper as shown in Fig. 7.

The results for constant drag should produce lines at a slope of 45°, called Constant Flow Lines. For convenience the reading corresponding to Zero Initial Tension or $H=0$, is taken from the diagram and referred to as h_0 .

The diagram illustrates some further interpretations that may be of use. For a constant initial tension the results would be expected to fall on the continuous curve so designated in the figure. The values of h_0

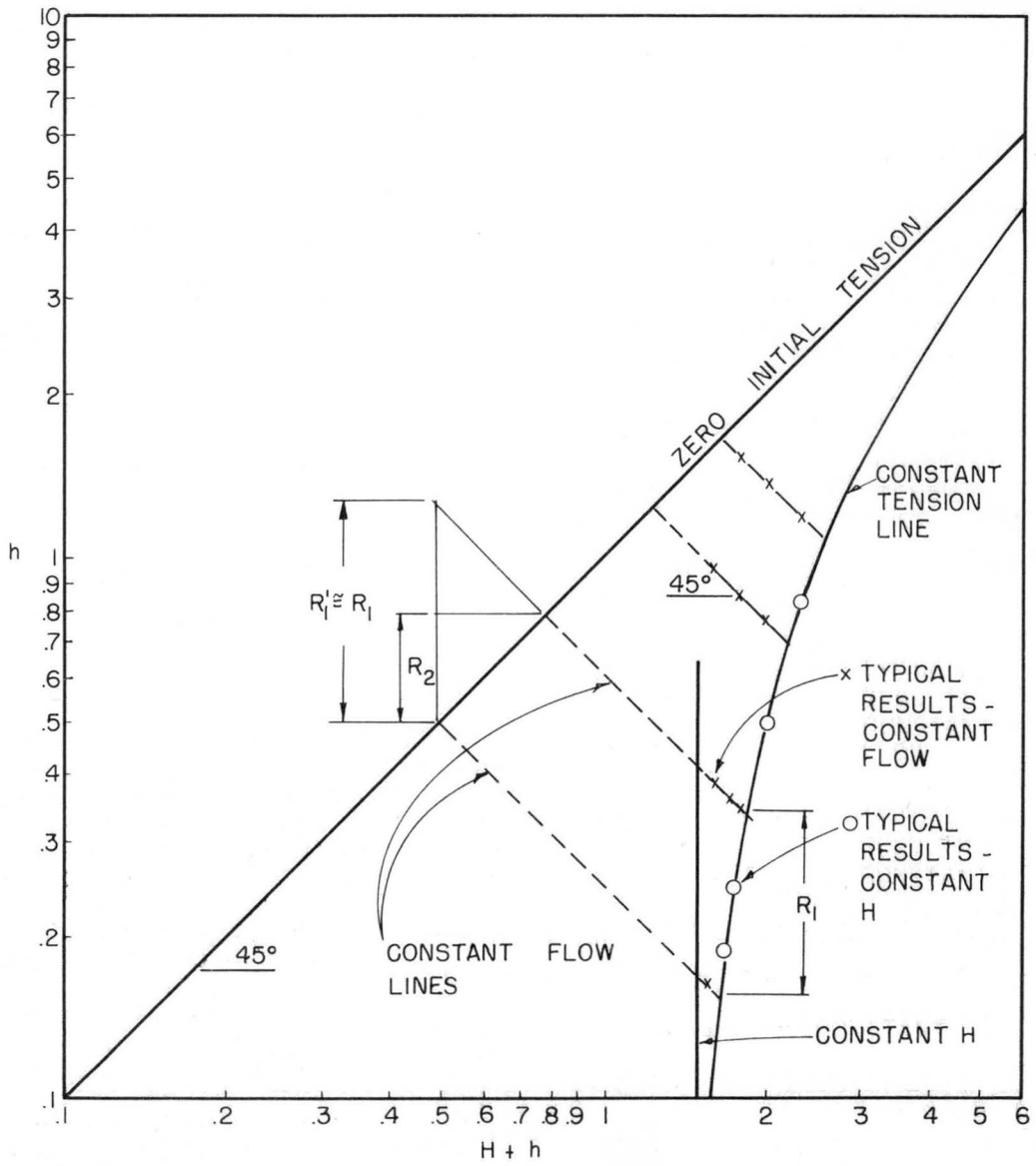


FIG. 7 GENERALIZED INTERPRETATION OF TEST RESULTS

can be derived as before by extension to the Zero Initial Tension line. An approximation is also possible (which may be made quite accurate) when it is seen that the relative value represented by R_1 is extracted as a drag reading R_2 which is the square root of R_1 . When $H \gg h$, R_2 is very closely the square root of R_1 . This situation might well allow the value of h_0 to be determined without the need for plotting the results.

D. Further Discussion of the Drag Integral

The procedure outlined so far enables the value of h_0 to be determined and from inspection of the Equation (11) for example, it would seem that the value of h_0^2 should be correlated with the drag integral.

Contrary to the previous situation where the effect of H was being studied for a constant Drag Integral, it seems now appropriate to accept the symmetry of the suspension wire and recognize that although the value of θ_A is varying as well as the value of h_0 , the sensing element only registers the magnitude of h_0 as the drag is varied.

The line integration performed by the wire will now be studied in more detail, including a critical examination of the meaning of the average velocity of the flow.

Referring to Fig. 6, the velocity u may be related to the distance from the wall y , for three types of flow in particular, namely;

- (a) Laminar Flow,
- (b) Turbulent Flow in a Smooth Pipe,
- and (c) Turbulent Flow in a Rough Pipe.

A brief description of these three types of flow is now included for the case of axisymmetric flow, together with an expression for the true average velocity for each one.

(a) Laminar Flow

Denoting shear stress τ , and the absolute viscosity μ the equilibrium of forces on a fluid cylinder of radius r and subjected to a pressure difference of Δp in a length L_1 may be expressed by the equation:

$$2 \pi r L_1 \tau = 2 \pi r L_1 \mu \frac{du}{dr} = \pi r^2 \Delta p$$

and integrated over the whole area of the flow, an expression for u_{\max} is

$$u_{\max} = \frac{\Delta p}{16 \mu L_1} D^2$$

Because the velocity distribution is parabolic, the values of u and u_{av} become:

$$u = \frac{\Delta p}{4 \mu L_1} \left(\frac{D^2}{4} - r^2 \right), \quad u_{\text{av}} = \frac{4}{\pi D^2} \int_0^{\frac{D}{2}} 2 \pi r u \, dr = \frac{\Delta p}{32 \mu L_1} D^2$$

(b) Turbulent Flow in a Smooth Pipe.

Representing the fluid density by ρ and the kinematic viscosity by ν , the wall shear stress is assumed to be

$$\tau_0 = \frac{f}{8} \rho u_{\text{av}}^2 = \frac{0.079}{2} \rho \nu^{1/4} D^{-1/4} u_{\text{av}}^{7/4}$$

The law of Blasius is taken as valid up to a value of Reynold's number (R) of 10^5 , f is a dimensionless friction factor and D the pipe diameter.

$$\Delta p = \frac{f L_1}{2 D} u_{\text{av}} = 0.158 L_1 \rho \nu^{1/4} D^{-5/4} u_{\text{av}}^{7/4}$$

Using F to denote a 'function of', the following arrangements of velocities can be applied

$$\frac{u}{u_{\max}} = F \left(\frac{\frac{D}{2} - r}{\frac{D}{2}} \right) = F \left(\frac{y}{\frac{D}{2}} \right) = \left(\frac{y}{\frac{D}{2}} \right)^n,$$

$$u_{\text{av}} = k_6 u_{\max} = k_7 \left(\frac{D}{y} \right)^n u$$

With these arrangements, eventually

$$u = k_8 \left(\frac{\tau_0}{\rho} \right)^{4/7} \nu^{-1/7} D^{1/7-n} y^n$$

Near the wall, because of the very local influence of the boundary layer, it is felt that the flow conditions would be independent of the diameter and therefore one can write

$$D^{1/7-n} = 1, \text{ that is, } n = \frac{1}{7}$$

This immediately leads to the seventh power law for the velocity distribution. It has been observed that this is also a good approximation for the central regions of the pipe as well. The values of u and u_{av} are,

$$u = 8.6 \left(\frac{\tau_0}{\rho} \right)^{4/7} \nu^{-1/7} y^{1/7} \quad \text{or} \quad u = k_9 y^{1/7}$$

$$\begin{aligned} u_{\text{av}} &= \frac{k_{10}}{\pi D^2} \int_0^{\frac{D}{2}} 2 \pi \left(\frac{D}{2} - y \right) y^{1/7} dy = \\ &= 7.00 \left(\frac{\tau_0}{\rho} \right)^{4/7} \nu^{-1/7} \left(\frac{D}{2} \right)^{1/7} \end{aligned}$$

(c) Turbulent Flow in a Rough Pipe

Referring to such texts as J. M. Kay (1957) this type of flow may be represented by an equation of the form,

$$u^* = A + B \log_e y^* ,$$

$$u^* = \frac{u}{\left(\frac{\tau_o}{\rho}\right)^{1/2}} ,$$

$$y^* = \frac{y}{\nu} \left(\frac{\tau_o}{\rho}\right)^{1/2} = k_{11} y$$

where A and B will depend on particular boundary conditions.

Integrating this expression leads to a form for the average as follows

$$u_{av}^* = -\frac{4}{\pi D^2} \int_0^D \pi \left(\frac{D}{2} - y\right) \left[A + B \log_e k_{11} y\right] dy =$$

$$= \left[A - \frac{3B}{2}\right] + B \log_e \frac{D}{2\nu} \left(\frac{\tau_o}{\rho}\right)^{1/2}$$

In all the cases above the average velocity was obtained by an integration of the form

$$I_a = \int f_1(u) r dr$$

which will be compared with the type of integration, I_w , associated with the suspension wire.

Calculating I_w for each of the three cases above results in an apparent average velocity as follows :

$$(a) 'u_{av}' = \frac{2}{D} \int_0^D \frac{\Delta p}{4 \mu L_1} \left(\frac{D^2}{4} - r^2\right) dr = \frac{\Delta p}{24 \mu L_1} D^2$$

$$(b) 'u_{av}' = 7.52 \left(\frac{\tau_o}{\rho}\right)^{4/7} \nu^{-1/7} \left(\frac{D}{2}\right)^{1/7}$$

$$(c) 'u_{av}^*' = (A-B) + B \log_e \frac{D}{2\nu} \left(\frac{\tau_o}{\rho}\right)^{1/2}$$

It appears that the integration of the type I_w for these three cases does not produce a form of 'average' velocity that is functionally different from the true average velocity in the case of axisymmetrical flow. There is a numerical difference however of which one should be wary in deriving the average velocity from information using such a device as a Pitot tube in a circular pipe, or the suspension wire principle.

It is not necessarily correct to assume that $f(u)$ bears a linear relation to $f_1(u)$, in fact if we

assume even the form

$$f(u) \propto [f_1(u)]^n$$

any number of complex relationships are possible for $1 < n < 2$.

The situation for $n = 2$ and for the three specific types of flow already considered has been evaluated and yields the following comparison between

$$I, \int f_1^2(u) r dr \text{ and } II, \int f_1^2(u) dr$$

$$(a) I, \frac{8}{6} u_{av}^2 ; II, \frac{32}{15} u_{av}^2$$

$$(b) I, \frac{74}{72} u_{av}^2 ; II, \frac{74}{63} u_{av}^2$$

$$(c) I, (u_{av}^*)^2 + \frac{5}{4} B^2 ; II, (u_{av}^*)^2 + B^2$$

Again it is apparent in this extreme that the final expressions do not provide forms that are functionally different for the two types of integration.

Although this has been limited it is felt that it would not be unreasonable to attempt a direct correlation between the drag result h_o and the average velocity or the Reynolds number for the wire R_w based on the true average velocity.

Finally, two facts should be noted, firstly in the case of two-dimensional flow or in the use of the suspension wire probe the appropriate average velocity ordinarily involves an integration of the form I_w and secondly it is clear from the assumptions that the suspension wire would be sensitive to asymmetry of the velocity profile.

E. The Influence of the Wire Characteristics

In order to compare the effect of the characteristics of the wires used it is necessary to consider the projected area of the wire, the degree of stretch and the type of velocity profile which is contributing to the drag on the wire.

For comparisons of the wires in the 2" nominal diameter conduits and the 11" x 5-1/2" water tunnel the value of h_o is modified in the following manner.

$$h_o \cdot \frac{1}{A_p} \cdot S_R \cdot F_v = h_o'$$

In the above expression, A_p is the projected area of the wire, that is, the product of the wire diameter and its exposed length. S_R is the ratio of the elongation of the wire to the beam deflection for an equal force and includes therefore the effect of the wire cross-sectional area and its total length. This term is included in this way because the value of h_o alone is used for correlation as discussed in D above and it is necessary to make an allowance for the order of magnitude of $\tan \theta_A$. The value of F_v is determined by the type of velocity distribution, F_v the apparent average velocity in the plane of the wire

and the true average velocity. It is based on a two-dimensional flow with a constant velocity over the wire length giving a value of F_v of unity.

The value of S_R is tabulated in Table I, and the values of F_v are included with the test result tabulations.

IV. TEST RESULTS

A. Conduit Studies

Three series of tests were conducted with the suspension wire completely across the conduit using several different types of wire as tabulated in Table I.

TABLE I
Wire data

Type	Material	Dia.(inches)	Assumed Modulus of Elasticity	S_R^*
W1	Copper	0.0044	17×10^6	.09
W2	W1 covered with fiberglass			
W3	Copper	0.0062	17×10^6	.04
W4	Platinum	0.001	31×10^6	.95
W5	Plastic	0.0047	6.2×10^5	2.1
W6	Plastic	0.0071	6.2×10^5	0.9
W7	Plastic	0.0065	6.2×10^5	1.1

* S_R $\frac{\text{Wire elongation}}{\text{Beam deflection}}$ for 2" nominal diameter conduit.

All the wires were used at some stage except type W2 from which W1 was prepared. A number of unsatisfactory tests resulted from the initial work where inconsistencies occurred because of unsatisfactory shielding for zero drag, abnormally stiff and distorted wire, or an excess of impurities in the water supply and inadequate cleaning of the wire. Most of the test results have been included, as the general trends lending some support to the theoretical treatment, may still be found in all tests.

Series I - 2.06" diameter brass conduit.

This installation comprised a self-contained circulating water system with a 2.06" diameter smooth brass conduit over 25 feet in length and near the downstream end as illustrated in Fig. 2 an expansion chamber housed a stagnation tube for velocity profile study. Just prior to this point the wire was installed and it has been assumed that the velocity profile at the beginning of the jet represented conditions at the wire. The true average velocity was determined at all times by means of a weigh tank downstream.

This modified value of h_o' will then be correlated against the value of Reynolds number for each test, using the average velocity of the flow in the plane of the wire for the evaluation of the Reynolds number.

In Fig. 8 the velocity distribution for a small range of conduit velocities is shown and it deviates very little from a Blasius profile, away from the wall.

The test results have been incorporated in Table II and plotted in Figs. 9, 10 and 11. The value h at $H = 0$, that is, the representation of the drag for zero initial tension, has been extracted from the appropriate figure and entered back in the table. An explanation of the numerical values of h and H will be given later.

These results show some scatter due partly to the fact that during these tests technique and control had not been perfected. The importance of the total $H + h$ reading had not been fully appreciated at this stage and the inability to see the wire to ensure cleanliness was also a contributing factor.

The analytical requirement that the constant flow lines should lie at an angle of 45° is satisfied in most cases, and after presenting the next series' results certain correlations will be attempted.

Series II - 2.04" diameter plastic conduit

This series of tests was conducted to check the work done with the brass conduit as the condition of the wire could be closely observed.

The velocity profile at the point of the installation of the wire is shown in Fig. 12 together with a sketch of the test layout. Water was supplied from the main laboratory sump by a 4" pump with throttled delivery entering the test section via a standpipe which helped to provide a stable flow. The average velocity was again measured at all times by use of a weigh tank.

The velocity profile was determined for a range of discharge by use of a small cylindrical pitot tube with upstream and downstream orifices. The tube was inserted through the same holes used for attachment of the suspension wire device.

A slight asymmetry of the average velocity profile is evident in Fig. 12, producing approximately 1-1/2% variation from the mean at a velocity ratio of 0.90. The profile approximates turbulent flow in a rough pipe and for a comparison a Blasius profile is also shown.

The results of the suspension wire tests have been included in Table III where three of the four

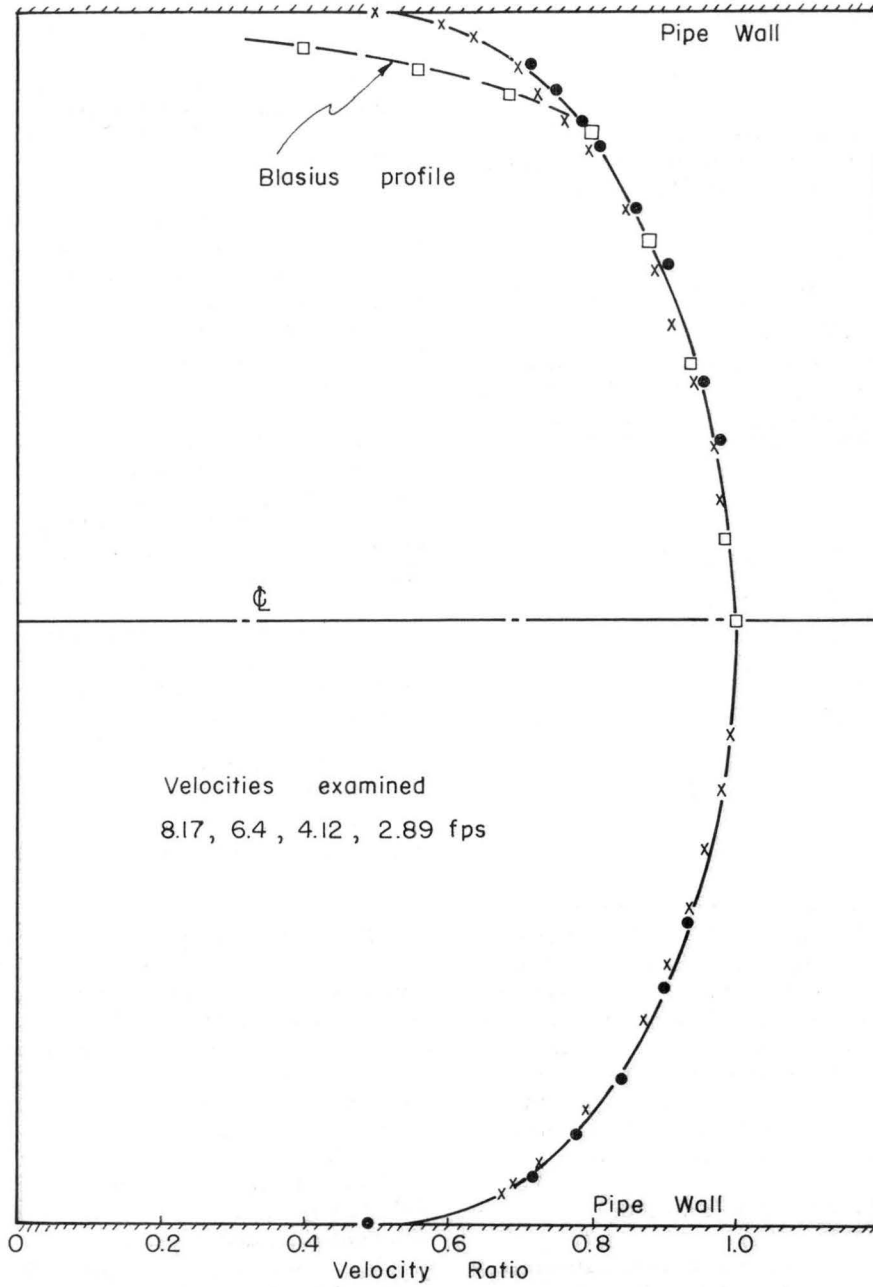


FIG. 8 VELOCITY DISTRIBUTION - 2.06" DIA. CONDUIT

TABLE II

2.06" dia. brass conduit $F_v = 1.07$

Wire H type	h	H + h	h _o	v f. p. s.	T °C	R _C x 10 ⁴	R _w						
W4	3.98	0.63	4.61	1.6	3.30	21.1	5.38	26					
	7.49	0.13	7.62										
	5.82	0.25	6.07										
	4.07	0.58	4.65	2.2	4.22	21.1	6.87	33					
	3.78	1.02	4.80										
	6.52	0.50	7.02										
	4.98	0.83	5.81										
	7.28	0.38	7.66										
	9.23	0.78	10.01	2.7	5.38	21.1	8.76	42					
	4.57	1.63	6.20										
	5.65	1.38	7.03										
	7.57	0.83	8.40										
	7.90	0.79	8.69										
	6.82	0.96	7.78										
	6.15	1.17	7.32						2.9	4.87	21.1	7.93	38
5.32	1.33	6.65											
W3	2.4	2.2	4.6	3.6	3.42	20.6	5.50	165					
	4.9	2.0	6.9										
	4.0	2.2	6.2										
	4.9	1.9	6.8	9.0	5.85	20.6	9.40	280					
	8.9	1.7	10.6										
	7.1	1.8	8.9										
	3.4	2.2	5.6										
	6.5	6.4	12.9										
	6.0	6.5	12.5										
	4.8	4.4	9.2						6.3	4.85	20.6	7.80	235
	7.5	4.2	11.7										
	2.9	4.8	7.7										
	4.2	4.6	8.8										
	7.6	7.1	14.7	9.6	6.21	20.6	9.98	300					
	6.6	7.2	13.8										
6.9	7.2	14.1											
4.5	7.4	11.9											
5.8	6.1	11.9	8.6						5.33	20.6	8.57	255	
8.9	5.5	14.4											
3.5	6.3	9.8	7.2						5.02	20.6	8.07	240	
4.4	5.1	9.5											
7.8	4.5	12.3											
5.9	4.8	10.7											
W5	5.4	5.4		10.8	7.8	7.04	21.1	11.5					260
	4.4	5.8	10.2										
	2.6	7.1	9.7										
	3.0	6.4	9.4	1.4	2.60	21.1	4.24	96					
	3.7	0.5	4.2										
	5.1	0.3	5.4										
	2.0	0.7	2.7										
	4.9	0.5	5.4										
	2.1	1.9	4.0						2.8	3.77	21.1	6.14	140
	3.0	1.7	4.7										
	4.6	1.3	5.9										
	4.1	1.4	5.5										
	4.2	3.1	7.3	4.8	5.27	21.1	8.58	195					
	3.0	3.5	6.5										
	5.1	2.8	7.9										

TABLE III

2.04" dia. plastic conduit $F_v = 1.01$

Wire H type	h	H + h	h _o	v f. p. s.	T °C	R _C x 10 ⁴	R _w									
W7	1.9	2.4	4.3	3.3	3.59	15.0	4.94	158								
	2.2	2.5	4.7													
	1.6	1.05	2.65	1.7	2.38	15.0	3.27	104								
	1.2	1.08	2.28													
	1.0	1.12	2.12													
	1.9	1.0	2.9													
	2.4	0.92	3.32													
	2.2	0.97	3.17	1.3	2.42	3.72	3.0	3.49	15.0	4.80	153					
	1.45	0.5	1.95													
	2.10	0.4	2.5													
	2.9	0.27	3.17													
	3.0	0.3	3.3													
	1.0	5.4	7.0									6.2*	5.67	15.0	7.80	249
	3.9	4.7	8.6													
	0.3	5.6	5.9	2.6	3.08	5.68	4.0*	4.45	15.0	6.12	195					
2.5	5.15	7.65														
0	3.92	3.92														
5.4	2.15	7.55														
2.0	3.10	5.10														
4.2	2.62	6.82	4.2	1.54	5.74	2.7*	3.35	15.0	4.60	146						
1.6	1.85	3.45														
1.9	1.73	3.63														
7.5	0.92	8.42														
5.3	1.23	6.57														
* Different bridge sensitivity and output range used																
W1	5.62	.58	6.20	1.9	2.83	15.0	3.9	84								
	5.15	.58	5.73													
	5.91	.53	6.44													
	6.28	.45	6.73													
	5.33	.61	5.94													
	6.22	1.0	7.22	2.4	3.27	15.0	4.5	97								
	5.65	.95	6.60													
	6.38	.69	7.07													
	6.50	.84	7.34													
	6.22	1.03	7.25						2.6	1.03	7.25	2.6	3.25	15.0	4.46	96
	5.78	1.05	6.83													
	5.39	1.13	6.52													
	6.44	1.0	7.44													
	6.50	.95	7.45													
	6.23	.90	7.13	4.50	1.21	5.71	5.21	1.05	1.92	15.0	2.63	57				
4.50	1.21	5.71														
5.21	1.05	6.26														
5.3	0.2	5.5														
6.03	.16	6.19														
4.62	.23	4.85	5.62	.21	5.83	4.90	.23	5.13	6.13	.66	6.79	2.1	2.72	15.0	3.73	80.5
5.62	.21	5.83														
4.90	.23	5.13														

TABLE III (continued)

Wire H type	h	H + h	h ₀	v f. p. s.	$\frac{\sigma^T}{C}$	$R_c \times 10^4$	R _w
W1	5.33	.74	6.07				
	6.13	.76	6.89				
	4.81	.80	5.61				
	6.05	.69	6.74				
	4.60	2.64	7.24	4.4	4.54	15.0	6.23 134
W6	2.10	0.50	2.6	1.2	1.97	15.5	2.76 96
	3.17	0.47	3.64				
	1.15	0.76	1.91				
	2.70	0.54	3.24				
	1.35	0.67	2.02				
	1.07	3.28	4.35	3.8	3.23	15.5	4.52 157
	0.66	3.46	4.12				
	0.66	0.76	1.42	1.25	1.93	15.5	2.70 94
	2.50	0.54	3.04				
	1.40	0.72	2.12				
	1.50	0.68	2.18				
	2.10	0.61	2.71				
	2.26	1.62	3.88	2.5	2.60	15.5	3.64 127
	1.10	1.95	3.05				
	1.00	2.02	3.02				
	1.60	1.84	3.44				
1.70	1.91	3.61					
1.90	1.80	3.7					
2.30	0.31	2.61	0.9	1.70	15.5	2.38 83	
2.05	0.36	2.41					

wires used were plastic. This preference arose because the plastic wire has much less lateral stiffness than the copper wire.

In Figs. 13, 14, 15 and 16 the data from Table III has been plotted and the value of h at $H = 0$ derived as before.

The results of both series of tests in the 2" nominal diameter conduits have been reproduced in Fig. 17 with the drag represented by h (at $H = 0$) as ordinate and Reynolds number for the wire as abscissa.

In all cases except wire W5 in the brass conduit and W6 in the plastic conduit it is possible to obtain quite reasonable correlation of the form

$$h_0 \propto (\text{average velocity})^{1.5}$$

In the case of W5 the exponent would be 1.75 and for W6 (although there is no line drawn) an exponent of approximately 2 would give the best fit.

In this plot in Fig. 17, no account has been taken of the projected area of the wire or the velocity distribution and so only comparisons of line slope can be made.

Series III - Water tunnel

In order to determine the effect of the wire diameter and length or more generally the effect of the

TABLE III (continued)

Wire H type	h	H + h	h ₀	v f. p. s.	$\frac{\sigma^T}{C}$	$R_c \times 10^4$	R _w
W6	1.05	0.51	1.56				
	1.50	0.40	1.9				
W5	5.06	6.44	11.5	8.5	7.67	14.5	10.4 240
	4.75	6.65	11.4				
	4.98	1.11	6.09	2.6	3.66	14.5	4.98 115
	2.21	1.87	4.08				
	2.48	1.72	4.20				
	3.09	1.48	4.57				
	3.85	1.23	5.08				
	4.11	0.66	4.77	1.9	2.99	14.6	4.07 95
	2.60	1.04	3.64				
	3.10	0.95	4.05				
	5.26	0.54	5.80				
	1.85	2.24	4.09	3.0	4.00	14.4	5.45 125
	3.6	1.68	5.28				
	3.5	1.8	5.3				
	2.68	2.07	4.75				
	3.6	1.1	4.7	2.2	3.11	14.5	4.23 100
	2.90	1.25	4.15				
	2.25	1.35	3.60				
	2.42	3.03	5.45	4.1	5.13	14.4	7.00 160
	1.64	3.25	4.89				
	2.9	3.0	5.9	4.2	5.05	14.3	6.88 160
	1.9	3.35	5.25				

projected area, a series of tests was conducted with the wire suspended across the 11" dimension of a 11" x 5-1/2" closed circulating water tunnel.

A pitot tube was incorporated in the tunnel at the upstream end of the working section so that it was possible to determine the velocity profile along the vertical centerline. This was the only means for determination of the average velocity in the circuit and so the reference velocity is that observed at the very center.

The wire was placed at the quarter point in the plane of the velocity measurement so as to avoid mutual interference and it is assumed that the velocity profiles for various flow rates, shown in Fig. 18, approximate the ones experienced by the wire.

Although there are some distortions of the velocity profile, within a percent or two one can assume a square profile for this series of tests.

The results have been tabulated in Table IV and reproduced in Figs. 19, 20 and 21 where the value of h at $H = 0$ has been determined by the usual construction.

In Fig. 22 the values of h_0 have been plotted against a Reynolds number for the wire based on the velocity at the center of the conduit.

In all cases it is possible to approximate the results by

$$h_0 \propto (\text{velocity})^{1.5}$$

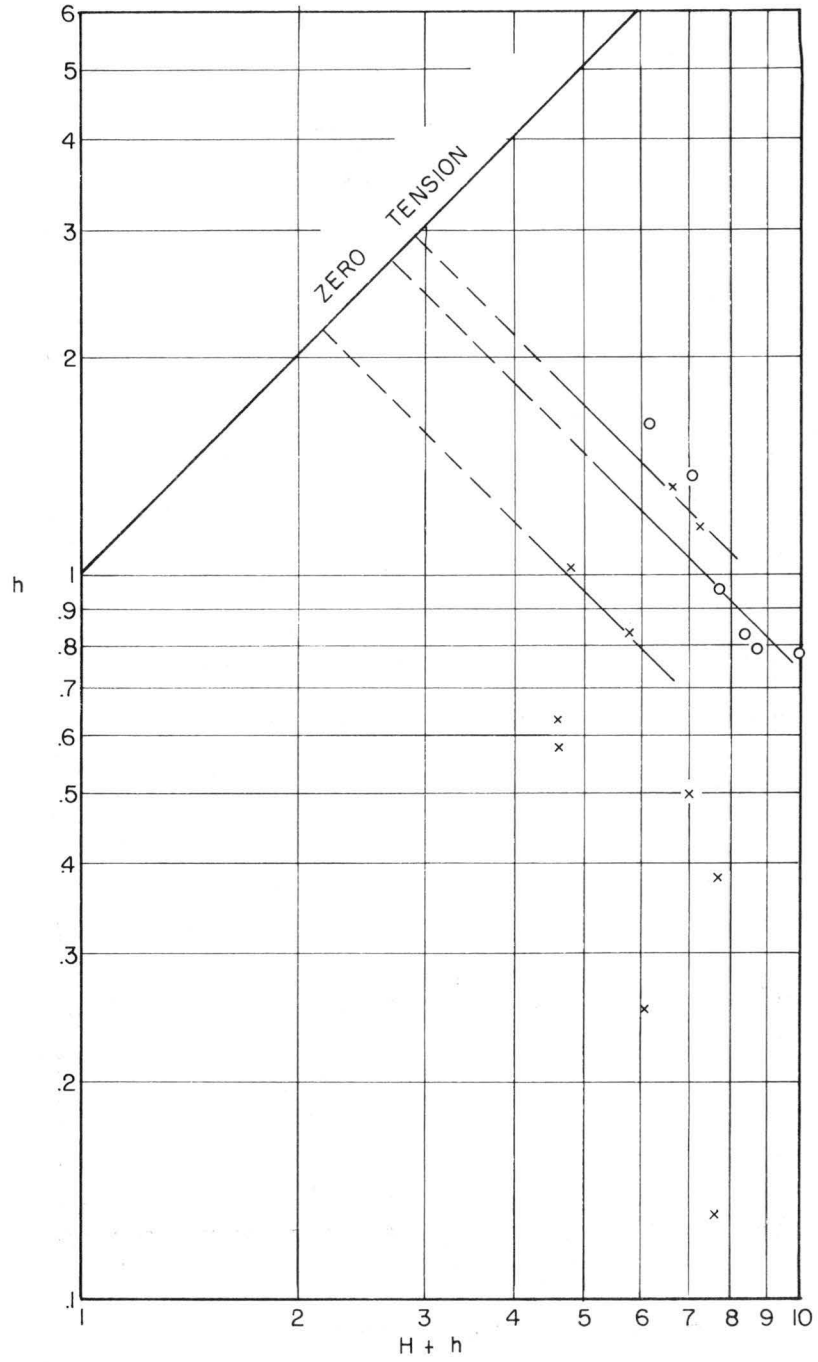


FIG. 9 W4 (Brass Conduit)

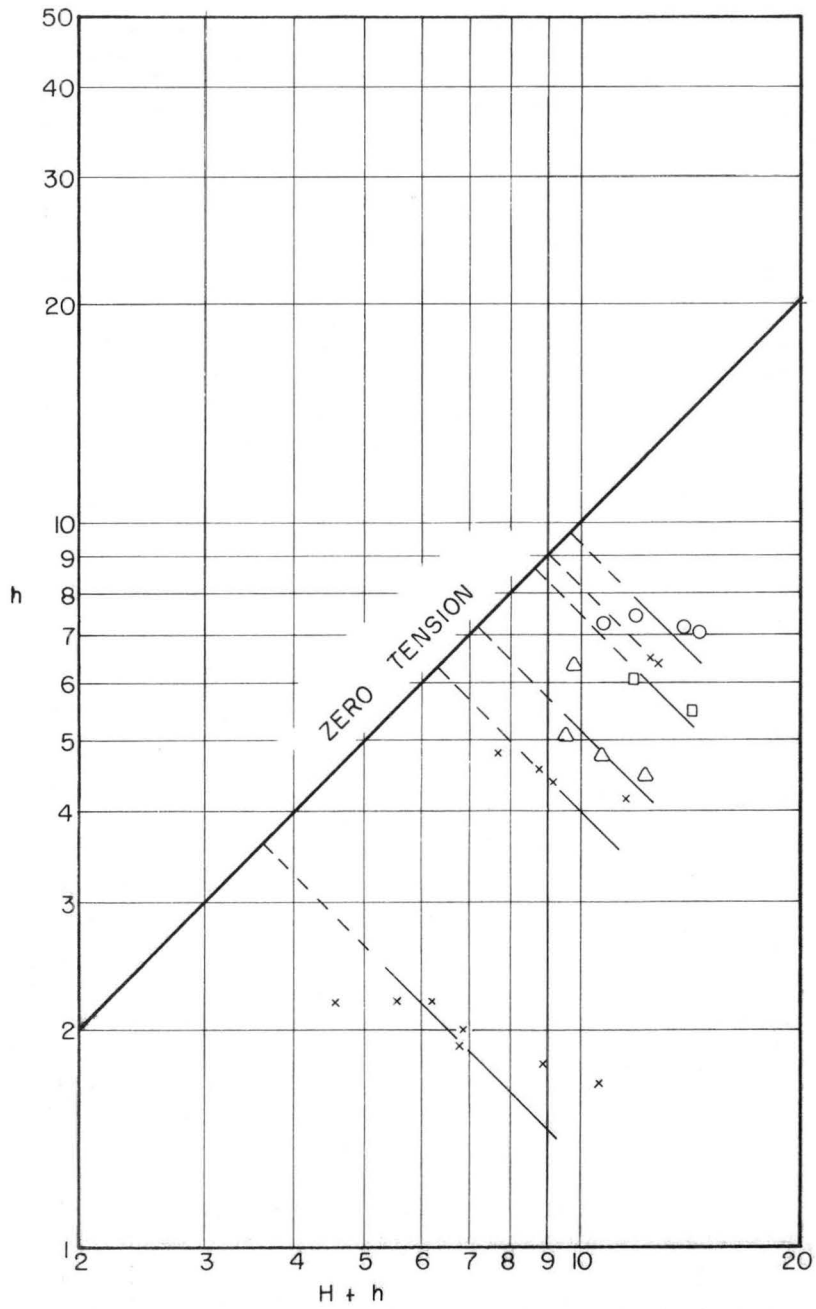


FIG. 10 W3 (Brass Conduit)

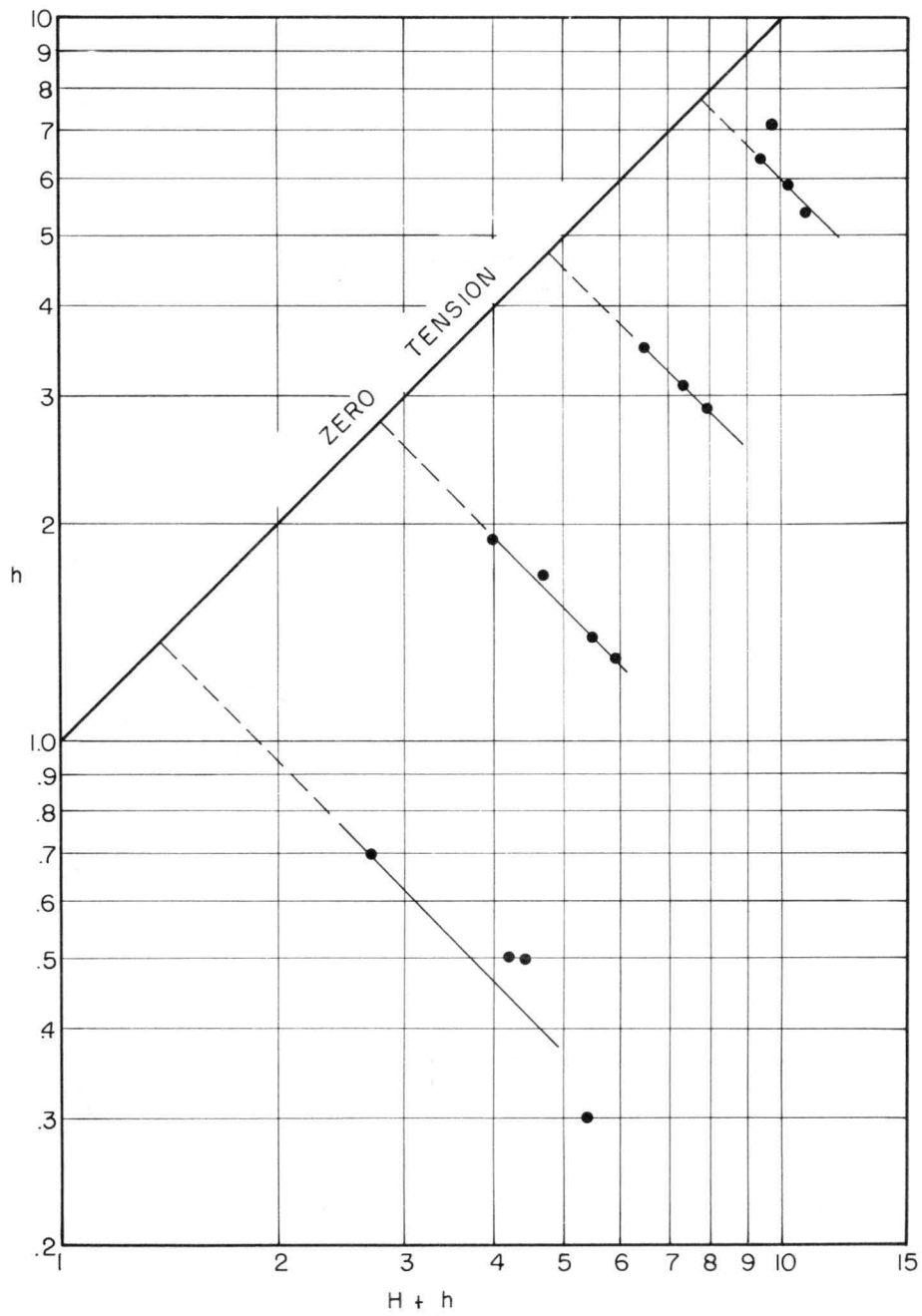


FIG. II W5 (Brass Conduit)

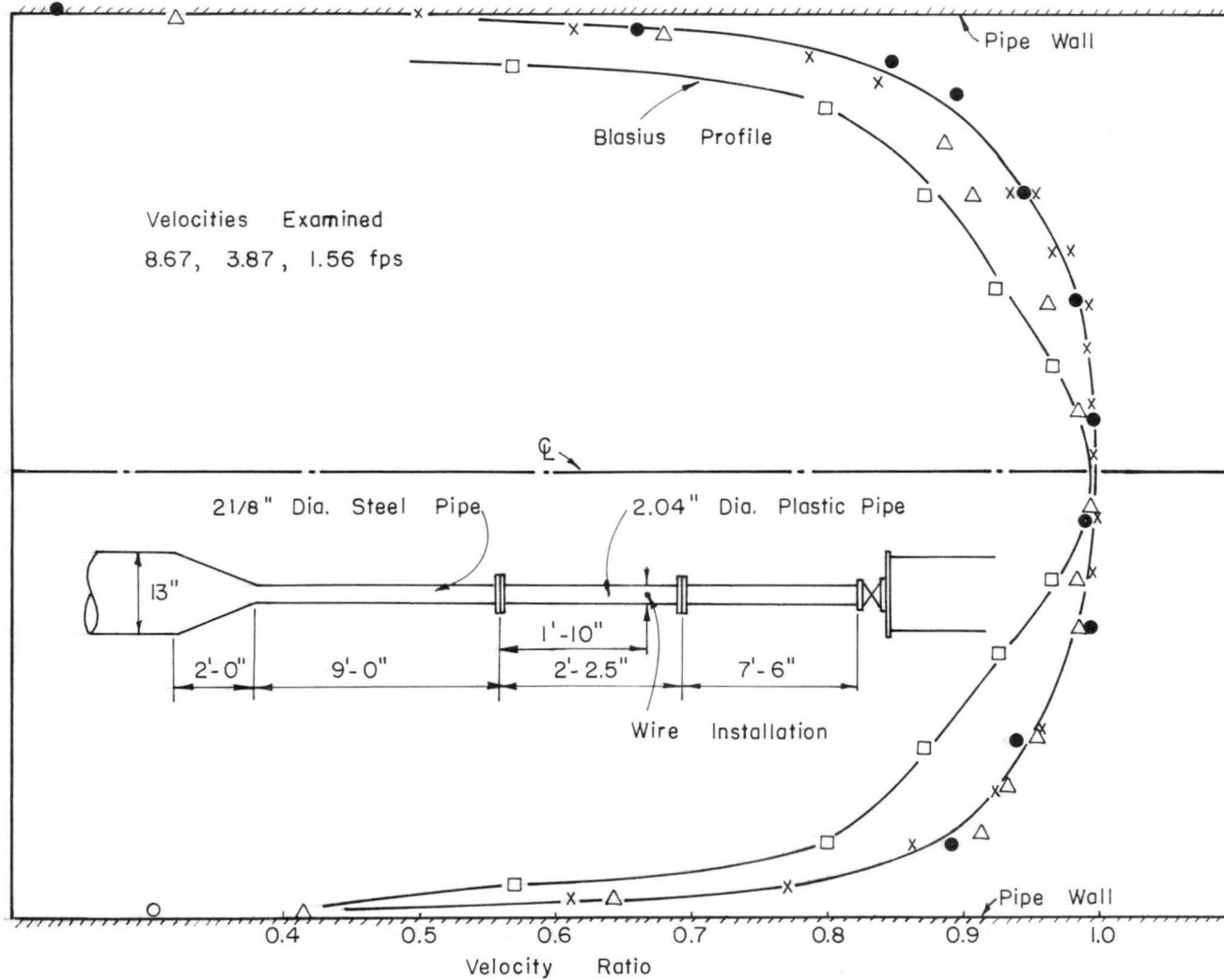


FIG. 12 VELOCITY DISTRIBUTION - 2.04" DIA. CONDUIT

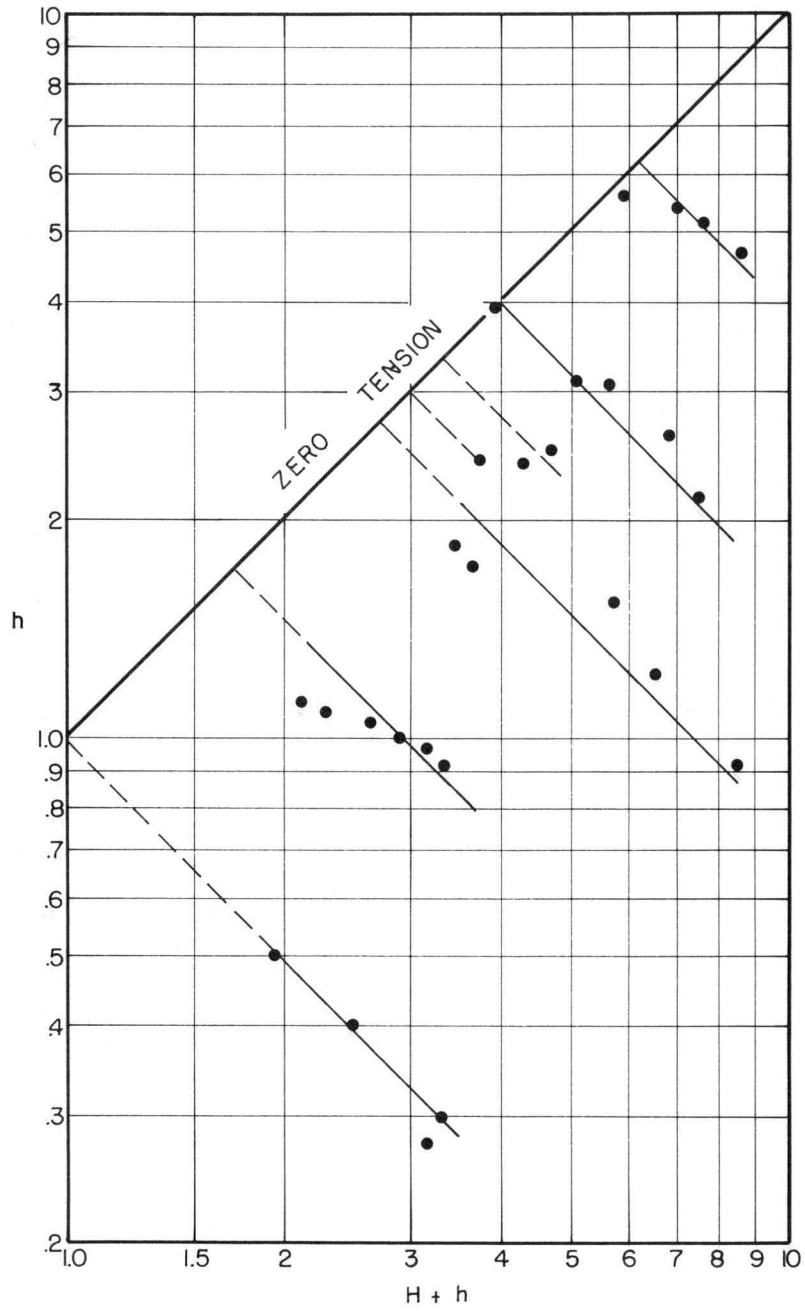


FIG.13 W7 (Plastic Conduit)

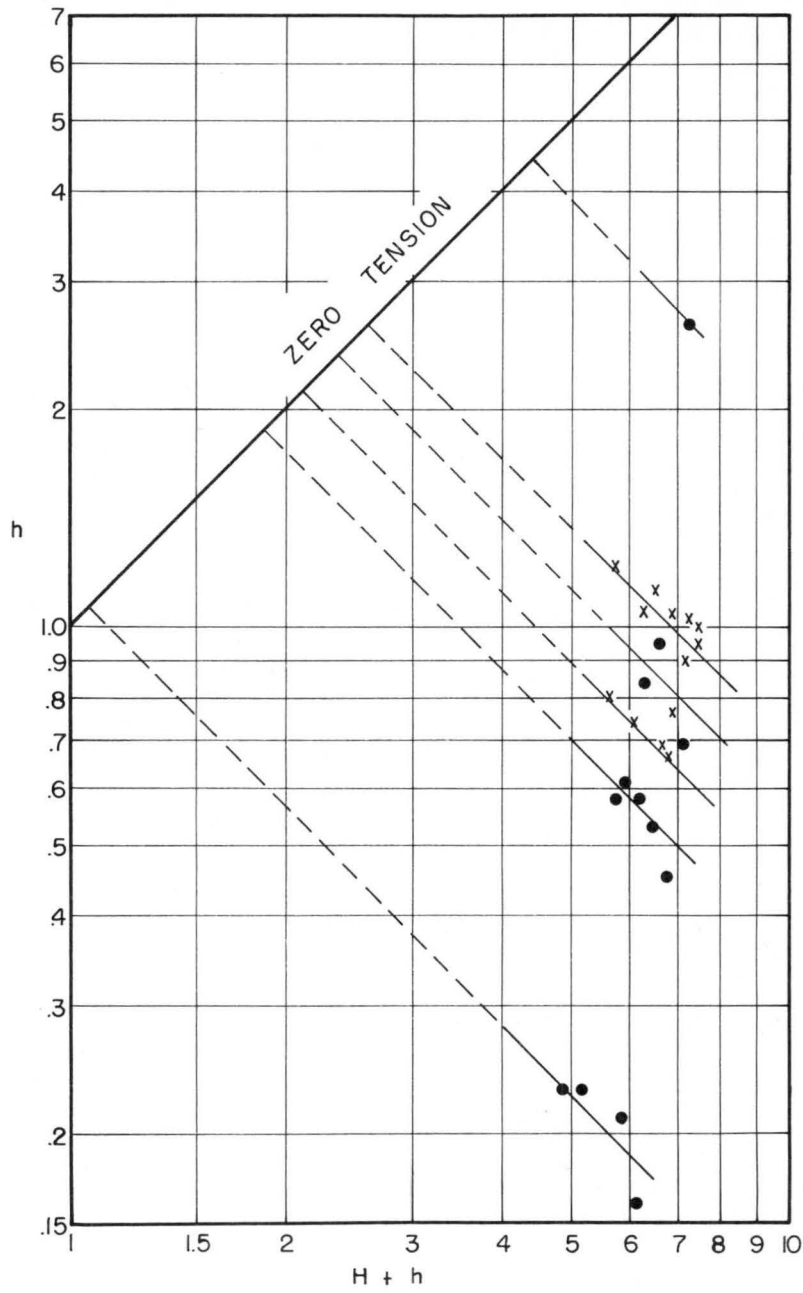


FIG. 14 WI (Plastic Conduit)

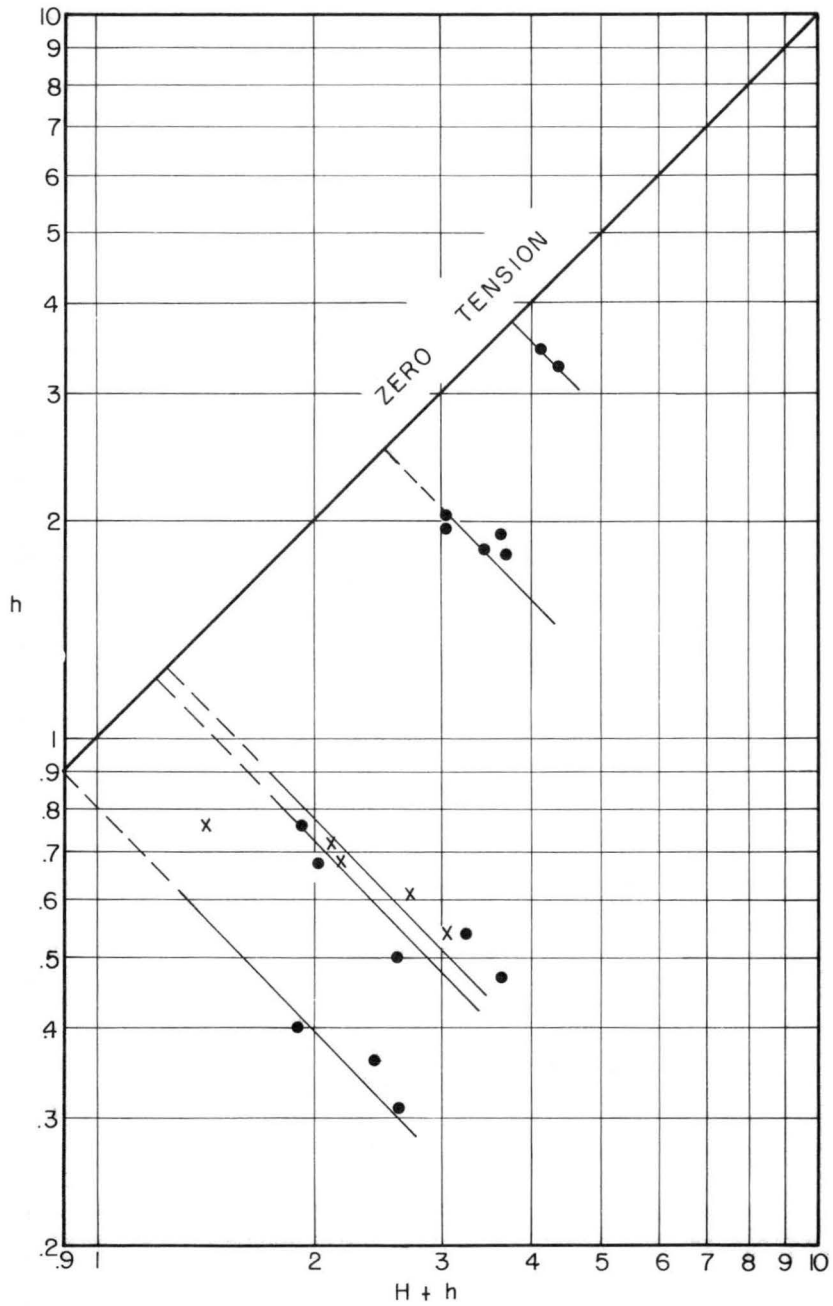


FIG. 15 W6 (Plastic Conduit)

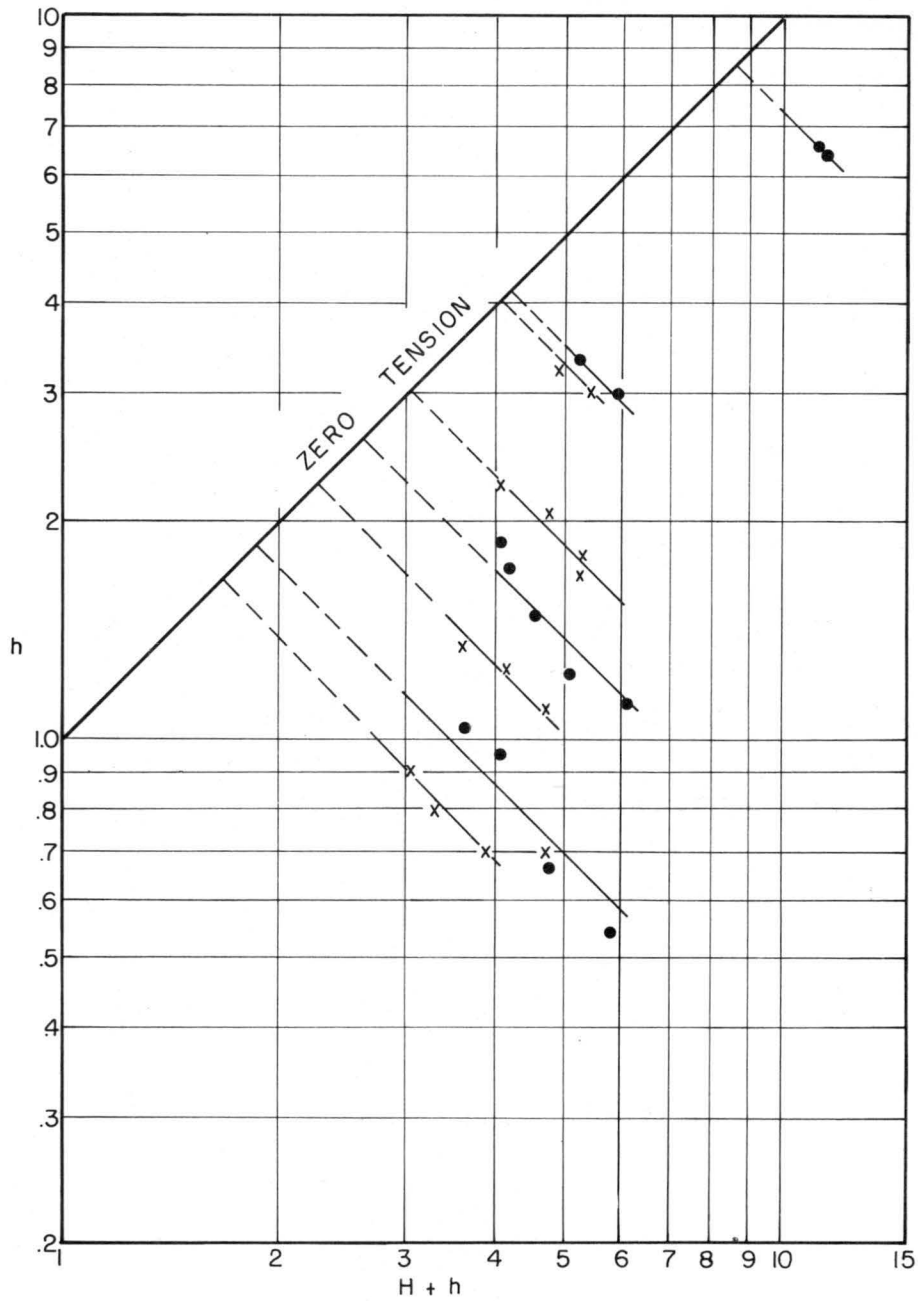


FIG. 16 W5 (Plastic Conduit)

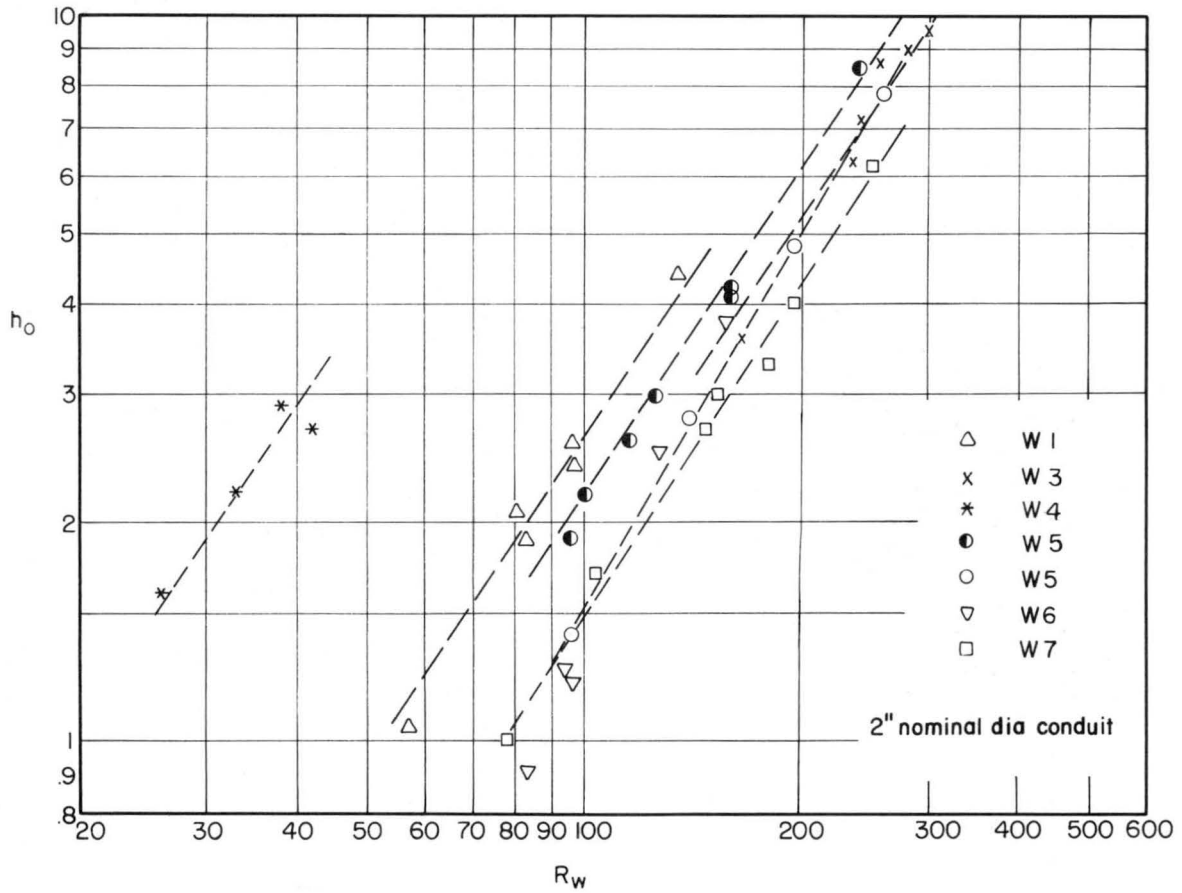


FIG. 17 CORRELATION OF TEST RESULTS WITH R_w

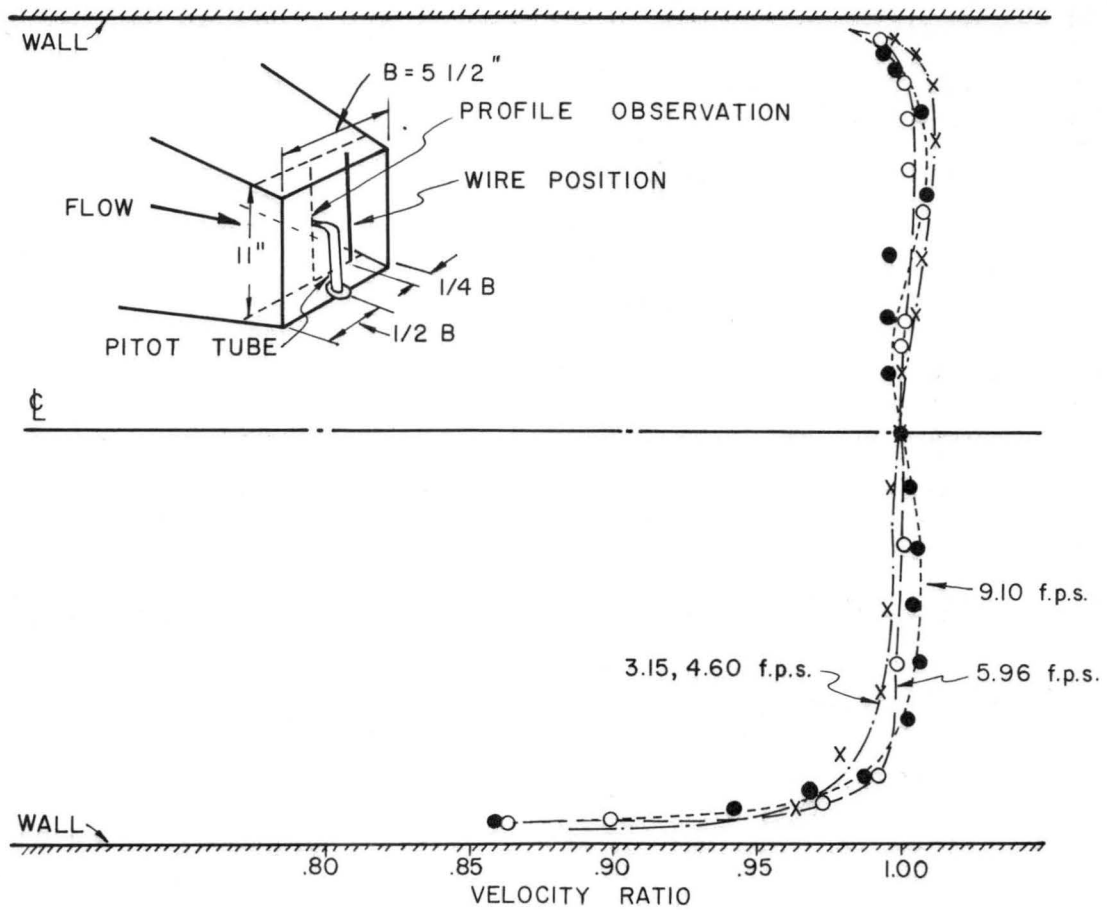


FIG. 18 VELOCITY DISTRIBUTION WATER TUNNEL

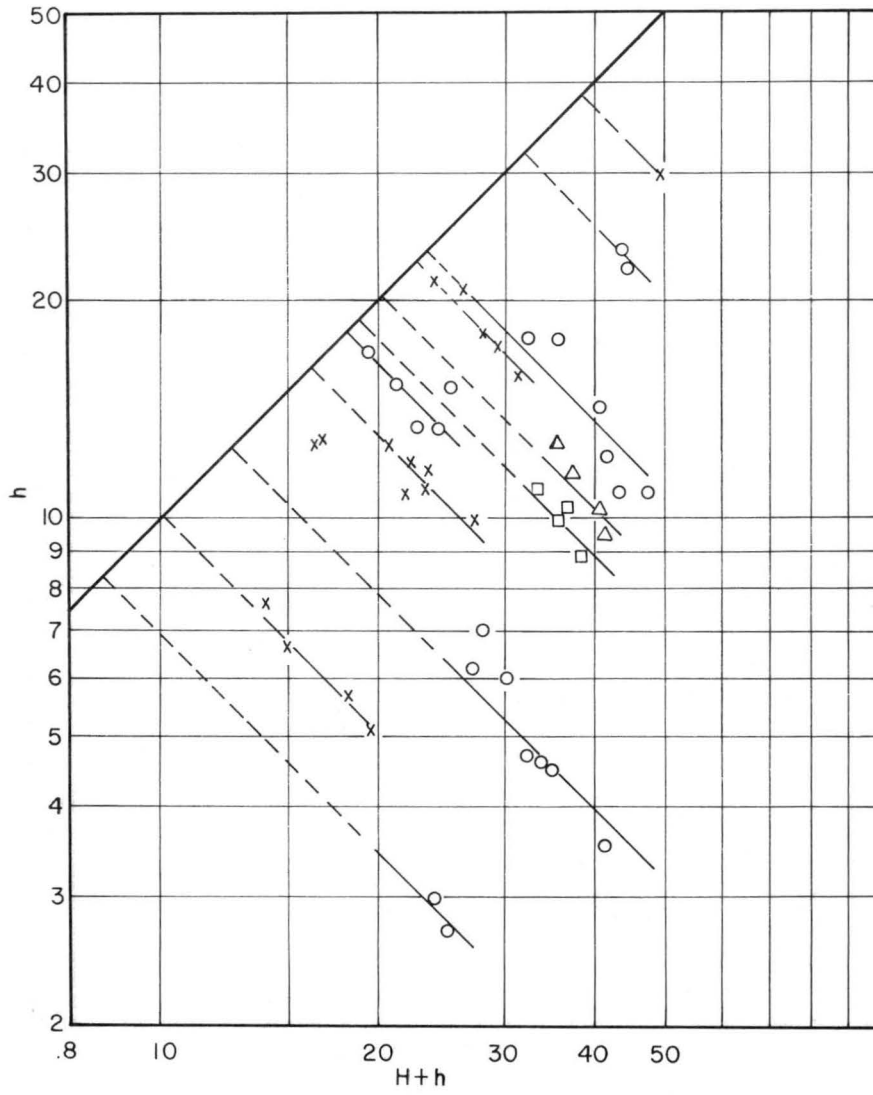


FIG. 19 W I (Water tunnel)

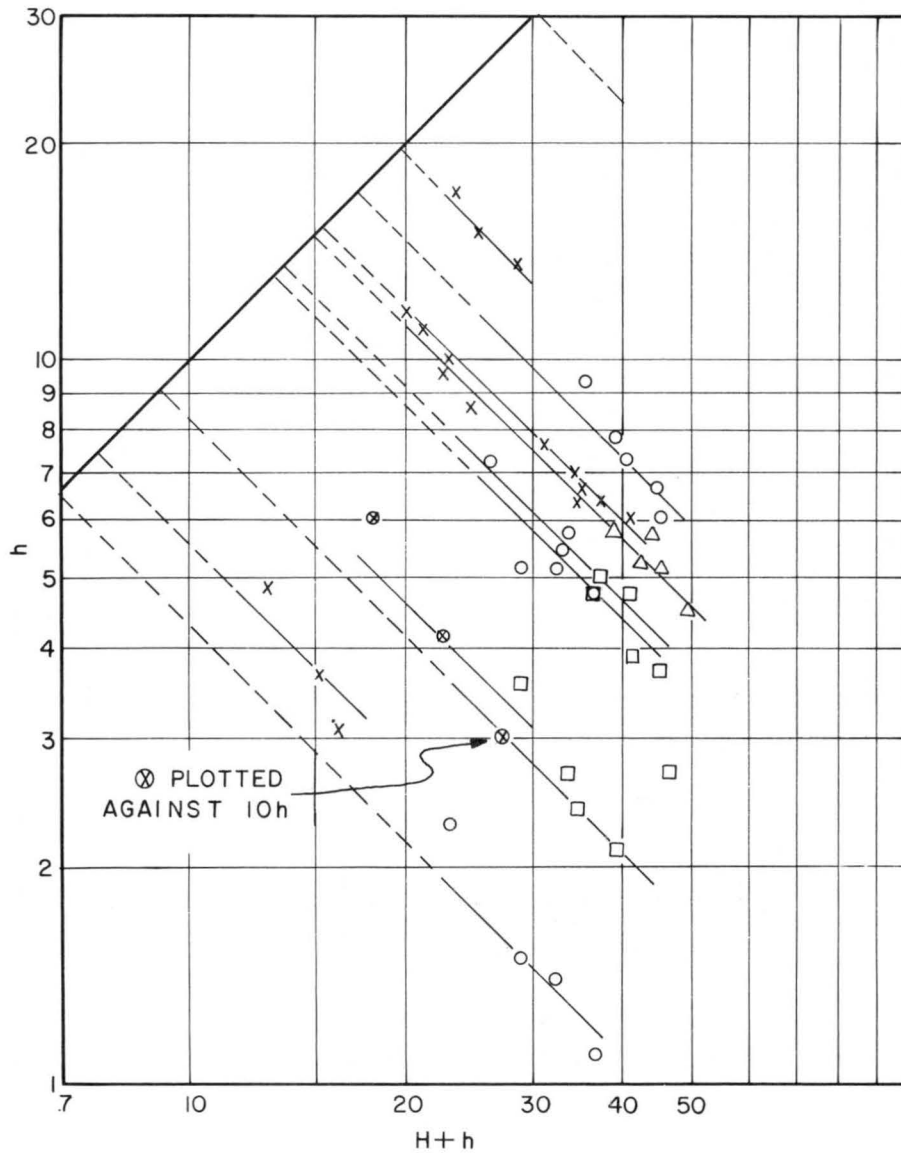


FIG. 20 W5 (Water tunnel)

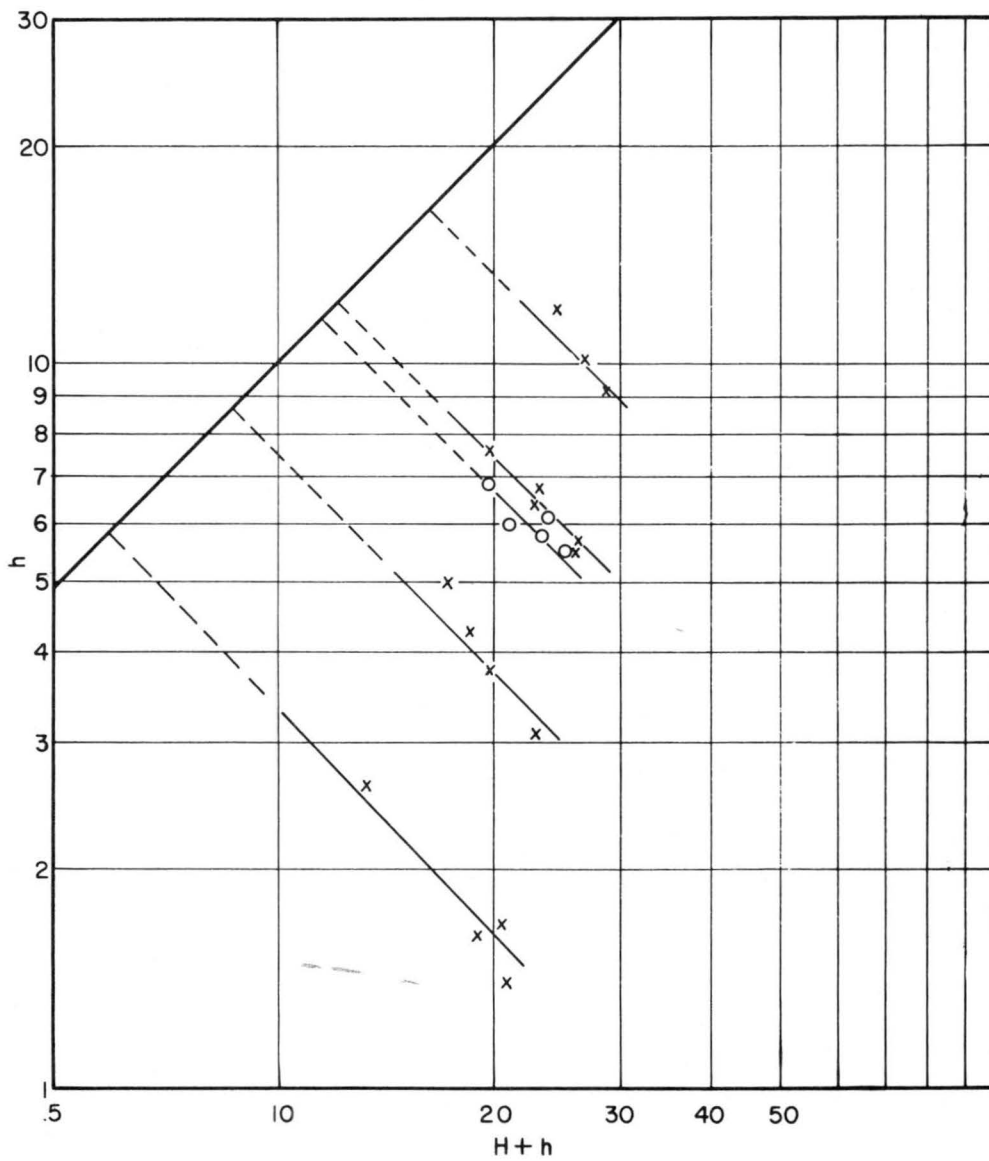


FIG. 21 W 6 (Water tunnel)

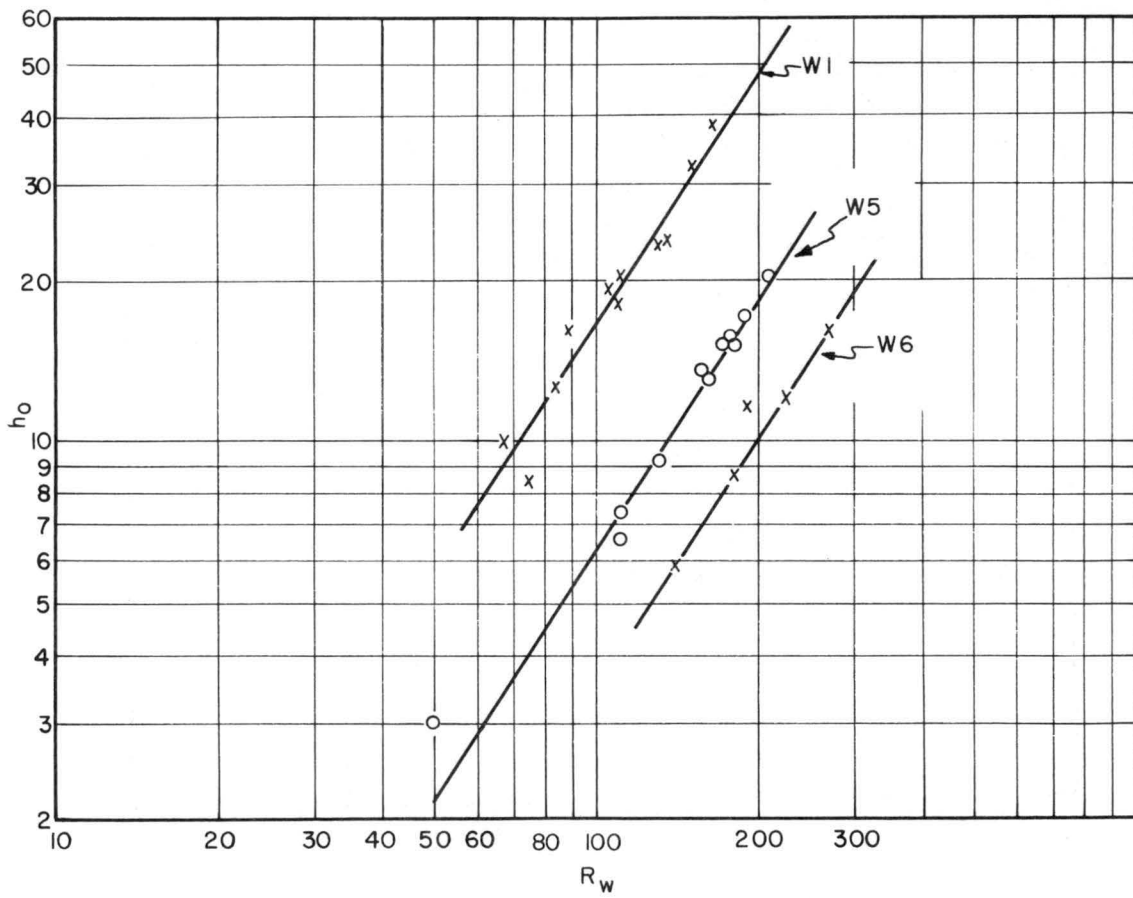


FIG. 22 WATER TUNNEL TESTS

TABLE IV

12" x 6" Water tunnel $F_v = 1.00$

Wire type	H	h	H + h	h_o	v_{max} f. p. s.	T_o °C	R_c $\times 10^5$	R_w					
W1	8.1	12.6	20.7	16	2.60	20.7	2.24	89					
	3.7	12.9	16.6										
	3.7	12.6	16.3										
	12.3	11.0	23.3										
	17.1	10.0	27.1										
	11.0	10.9	21.9										
	12.0	11.7	23.7										
	10.3	12.0	22.3										
	8.3	6.7	15.0						10	1.95	20.7	1.68	67
	14.6	5.1	19.7										
	6.3	7.7	14.0										
	12.6	5.7	18.3										
14.3	13.4	27.7	18	3.11	20.7	2.68	110						
5.7	15.4	21.1											
10.9	13.4	24.3											
10.0	15.1	25.1											
2.4	17.0	19.4											
15.4	15.7	31.1	23	3.75	20.7	3.24	130						
5.7	20.6	26.3											
12.0	17.2	29.2											
10.0	18.0	28.0											
2.6	21.3	23.9											
14.6	17.6	32.2	23.5	4.01	20.1	3.41	135						
18.1	17.6	35.7											
26.0	14.2	40.2											
36.5	10.8	47.3											
29.7	12.2	41.9											
32.7	10.8	43.5											
22.4	2.7	25.1	8.4	2.25	19.2	1.87	75						
21.1	3.0	24.1											
25.5	11.6	37.1	20	3.42	18.6	2.81	110						
32.4	9.2	41.6											
22.7	12.8	35.5											
30.0	10.3	40.3											
29.6	4.6	34.2	12.5	2.59	18.2	2.11	84						
30.5	4.5	35.0											
24.1	6.0	30.1											
37.6	3.5	41.1											
28.8	4.7	32.5											
21.1	6.2	27.3											
21.1	7.0	28.1											
20.0	29.8	49.8						38	5.12	18.2	4.16	165	
22.7	22.2	44.9											
20.0	23.5	43.5	32	4.63	18.2	3.77	150						
22.7	22.2	44.9											
22.4	11.1	33.5	19	3.28	17.9	2.64	105						
25.7	10.4	36.1											
25.5	10.0	35.5											
29.2	8.9	38.1											
W5	8.1	4.9	13.0	7.4	2.94	20.5	2.53	110					
	11.4	3.7	15.1										
	13.1	3.1	16.2										
	12.9	10.0	22.9	15	4.66	20.5	4.01	170					
	16.0	8.6	24.6										
13.0	9.7	22.7											

TABLE IV (continued)

Wire type	H	h	H + h	h_o	v_{max} f. p. s.	T_o °C	R_c $\times 10^5$	R_w					
W5	8.1	11.9	20.0	20	5.69	20.5	4.89	210					
	10.0	11.1	21.1										
	10.0	15.1	25.1										
	6.3	17.2	23.5										
	14.9	13.7	28.6										
	22.3	0.42	22.7						3.0	1.42	18.2	1.15	49
	17.7	0.61	18.3										
	27.1	0.30	27.4										
	27.7	5.5	33.2						13	4.58	18.2	3.73	160
	31.4	4.8	36.2										
	23.8	5.2	29.0										
	18.9	7.3	26.2										
27.7	5.2	32.9											
32.8	7.3	40.1	17	5.58	18.2	4.54	190						
39.2	6.1	45.3											
38.0	6.7	44.7											
31.9	7.9	39.8											
26.8	9.4	36.2											
31.0	1.4	32.4						6.6	3.25	17.9	2.62	110	
35.9	1.1	37.0											
20.7	2.3	23.0											
27.4	1.5	28.9											
25.3	3.6	28.9	9.2	3.84	17.9	3.10	130						
30.6	2.7	33.3											
32.5	2.4	34.9											
37.1	2.1	39.2											
35.2	6.1	41.3	15.5	5.11	17.9	4.12	175						
28.6	6.7	35.3											
23.4	7.7	31.1											
27.4	7.0	34.4											
30.7	6.4	37.1											
28.3	6.4	34.7											
37.3	3.9	41.2	13.5	4.30	20.0	3.65	155						
36.7	4.8	41.5											
32.1	5.0	37.1											
31.8	4.8	36.6											
27.9	5.8	33.7											
44.2	2.7	46.9											
41.2	3.8	45.0											
44.6	4.5	49.1						15*	4.99	20.0	4.23	180	
40.6	5.2	45.8											
39.1	5.8	44.9											
37.0	5.3	42.3											
34.2	5.8	39.0											
W6	19.5	1.4	20.9	5.9	2.40	22	2.14	140					
	10.7	2.6	13.3										
	14.3	1.9	16.2										
	18.8	1.7	20.5										
14.3	4.3	18.5	8.7	3.15	22	2.80	180						
19.8	3.1	22.9											
16.0	3.8	19.8											
11.7	5.0	17.2											
12.1	7.6	19.7						12	3.9	22	3.47	225	
16.4	6.7	23.1											

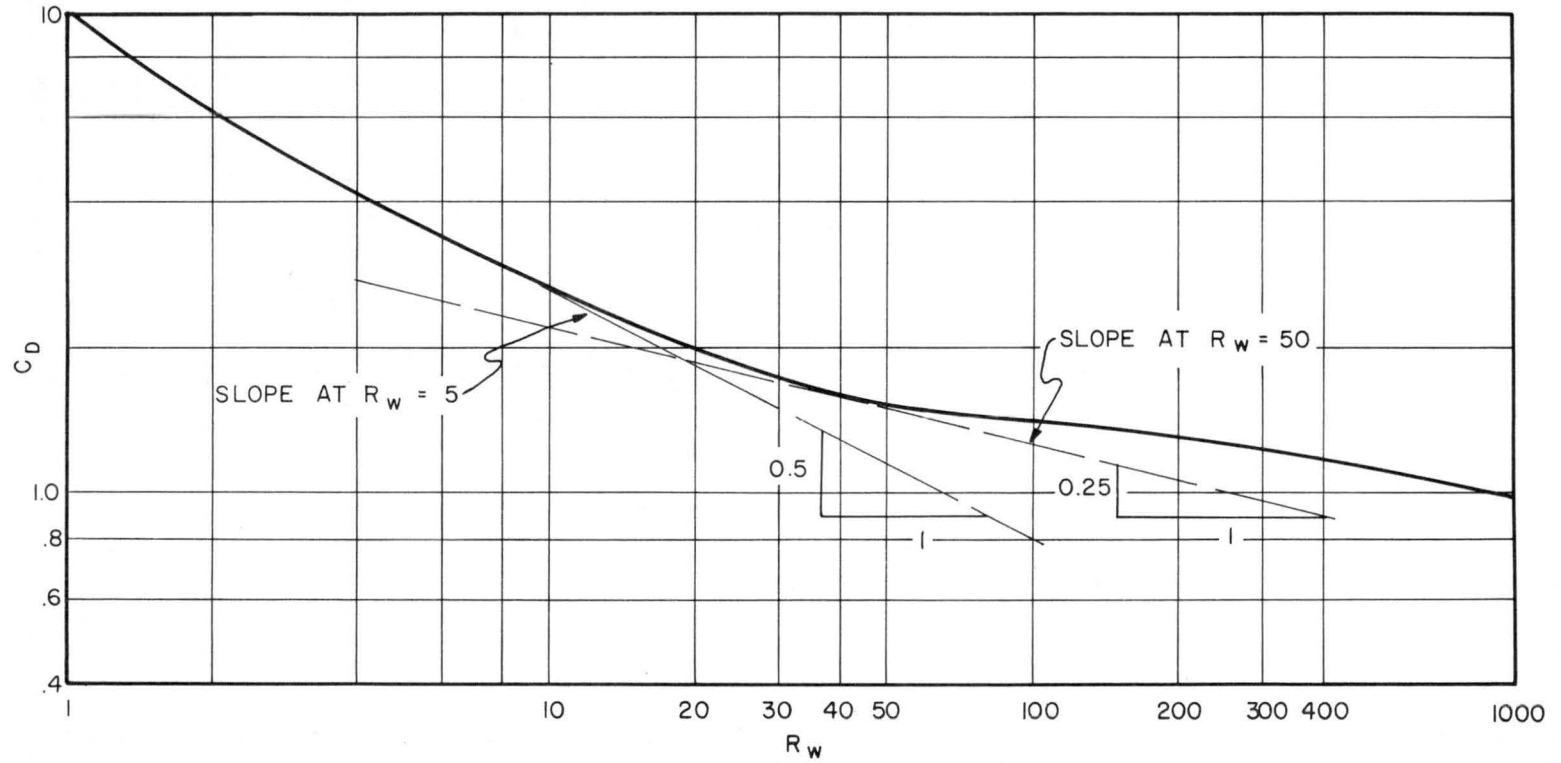


FIG. 23 DRAG ON FIXED CYLINDERS, INFINITE LENGTH
(WIESELSBERGER)

TABLE IV (continued)

Wire type	H	h	H + h	h ₀	v _{max} f. p. s.	o ^T C	R _C x 10 ⁵	R _w
W6	20.5	5.5	26.0					
	19.5	9.2	28.7	16	4.75	22	4.23	270
	12.6	11.9	24.5					
	16.4	10.2	26.6					

Series I, II, III - Comparisons

As it is now proposed to compare the three series the value of the units used for h and H and subsequently h₀ should be explained.

The calibration of the beam was performed at regular intervals in order to maintain a check on the elastic properties of the system and gram weights were used for this purpose. The readings on the meter were available in centimeters and as it was anticipated that the drag would be eventually evaluated the units of h, H and h₀ were recorded as gram units.

There are two reasons, however, why the units have not been shown in the test result tabulations and in the figures. Firstly, the tests were only qualitative and thus the readings are only considered accurate to within 5 and 10%, although from the point of view of studying the device the measurements served to indicate to a greater accuracy the stability and reliability of the results. Secondly, a further analytical study, not presented here, showed that evaluation of the absolute drag and eventually perhaps velocity would not be advisable until more accurate results are available, particularly as the solution involves a transcendental equation and hence trial and error methods for solution.

Before producing a composite of the results it seems the general trend for most of the tests in the conduits is to produce a relation of the kind:

$$h_0 \propto R_w^{1.5}$$

Referring to Fig. 23 which shows a portion of the results of the investigations of Weiselsberger from Prandtl and Tietjens (1957) for the coefficient of drag on fixed cylinders, it appears as though this coefficient varies approximately as R^{-1/2} and R^{-1/4} for values of R of 5 and 50 respectively.

This means that the drag on fixed cylinders for this range would be a function of the Reynolds number raised to the power 1.5 to 1.75, and as the Reynolds number is increased the exponent tends to a value of 2.

Although it has already been observed that the problem of the suspension wire is much more complex than that of the fixed cylinder, it is interesting

TABLE IV (continued)

Wire type	H	h	H + h	h ₀	v _{max} f. p. s.	o ^T C	R _C x 10 ⁵	R _w
W6	19.9	5.5	25.4		11.5	3.47	20.6	2.99
	17.8	6.1	23.9					190
	15.0	6.0	21.0					
	17.5	5.8	23.3					
	13.1	6.8	19.9					

that the relation obtained above approaches so nearly the case of a fixed cylinder.

In order to obtain some idea of the influence of the wire characteristics, the modified relative values of h' for each Series have been calculated as indicated in the General Analysis, under E.

The aggregate of the results is then included in Fig. 24, showing the various wire types with a subscript indicating the nominal size of conduit from which the result was obtained.

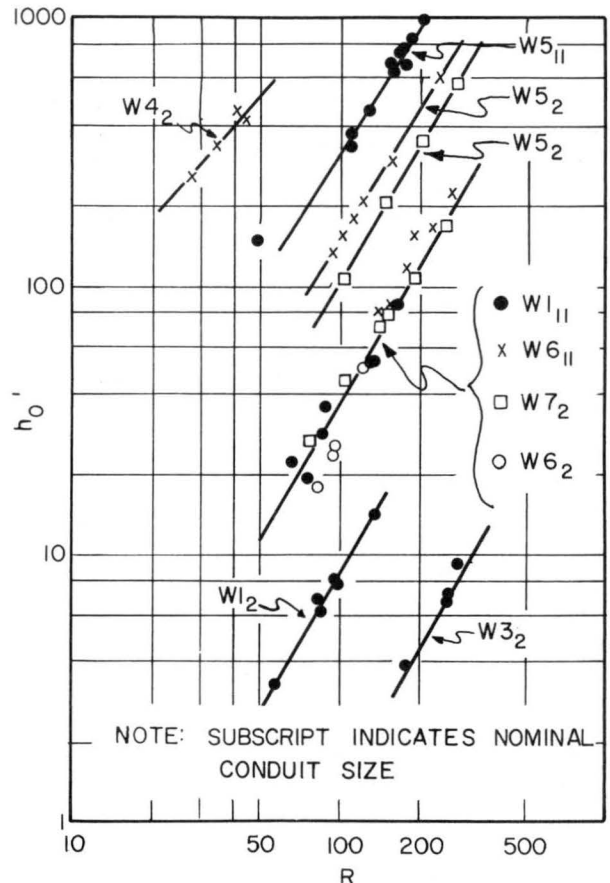


FIG. 24 INFLUENCE OF WIRE CHARACTERISTICS

If all factors had been satisfactorily allowed for, the results might have all fallen on one straight line instead of several groups.

Certain experimental trends were observed that would explain some of the differences and support the belief that the greatest contributing factor was the presence of considerable lateral stiffness in the wires used.

For example the copper wire in the short length of a nominal 2", that is W1₂ and W3₂, was found to be too stiff for practical use and only the thin copper in the water tunnel, W1₁₁, seemed to have desirable flexibility and in fact is considered superior to the plastic for such a length. The platinum wire is considered a special case as well, because of its size and low range of Reynolds numbers.

The remaining two groups indicate on the one hand that the analytical approach in the case of W₁, W₆, and W₇ is satisfactory whereas on the other hand the thin plastic W₅ shows some inconsistencies. One plausible explanation for this would be the difficulty of producing a uniform plastic material in a diameter as small as this. In general it is considered that the results are encouraging as the materials were rather randomly selected without any proper control on uniformity.

B. Suspension Wire Probe

The suspension wire probe was used in an 8" wide tilting flume to study the velocity distribution along the central vertical. Separate tests with a Prandtl tube showed that the velocity distribution across the central quarter of the flume varied by no more than $\pm 2-1/2\%$ and so for a qualitative investigation two-dimensional flow was assumed and only the

velocity distribution on the centerline will be included.

As it was established that the probe behaved extremely well in the flume and did not always necessitate rotation of the probe for the purpose of a zero check, it was decided to investigate conditions as close to the floor as possible. For this a false floor was installed and grooves to match the fork of the probe cut at the downstream brink. The probe could then be lowered until it was within a wire diameter of the floor and readings observed.

In Fig. 25 is shown the results plotted on log log and from which the value of h_0 has been derived and entered with other data in Table V. Also included for comparison in the table is the value of the square root of relative meter reading. As described in the analysis this latter value might serve as a good approximation for the drag reading.

The results show readings of drag down to 1/1000 foot from the floor. In the presentation of the results the accuracy of the work has been purposely underestimated because the accent is on qualitative behaviour and consequently the extrapolation of the drag-velocity relation in Fig. 26 and subsequently plotting in Fig. 27, is merely meant to be indicative of the procedure that might be necessary in applying this technique.

The ease and rapidity with which the tests were performed and the consistency of the results suggest that with suitable improvements of the equipment as a whole, measurements very close to the boundary may be possible.

TABLE V
Results of flume test - suspension wire probe drag measurements

Feet Depth	% Depth	h_0	% (h_0)	% Velocity	Meter Reading r	$\sqrt{\frac{r}{r_{max}}}$ x 100
0.016	8	0.45, 0.46	64	80.5	1.4, 1.5	68, 71
0.010	5	0.40, 0.42	58	76	1.1, 1.2	61, 63
0.007	3.5	0.33, 0.35	48		0.8, 0.9	52, 55
0.005	2.5	0.31	44		0.7	48
0.003	1.5	0.20, 0.23	30		0.3, 0.4	32, 36
0.002	1	0.17	24		0.2	26
0.001	0.5	0.12	17		0.1	18
0.002	1	0.12	17		0.1	18
0.005	2.5	0.31	44		0.7	48
0.008	4	0.42	59		1.2	63
0.015	7.5	0.46, 0.48	66	80	1.5, 1.6	71, 73
0.025	12.5	0.53	75	86	1.9	80
0.045	22.5	0.61, 0.60	85	93	2.3	88
0.005	2.5	0.36, 0.37	51		1.0, 0.9	58, 55
0.003	1.5	0.29	41		0.6	45
0.002	1	0.16	22.5		0.2	26
0.015	7.5	0.49	69		1.6	73
0.035	17.5	0.56	79	90	2.0	82
0.065	32.5	0.62, 0.64	89	96	2.4, 2.5	89, 91
0.105	52.5	0.65, 0.67	93	99.5	2.6, 2.7	93, 95
0.155	77.5	0.68, 0.71	97	100	3.0, 2.8	100, 97
0.175	87.5	0.71, 0.70	99	100	2.8, 2.9	97, 98
0.105	52.5	0.65, 0.67	93	99.5	2.6, 2.7	93, 95

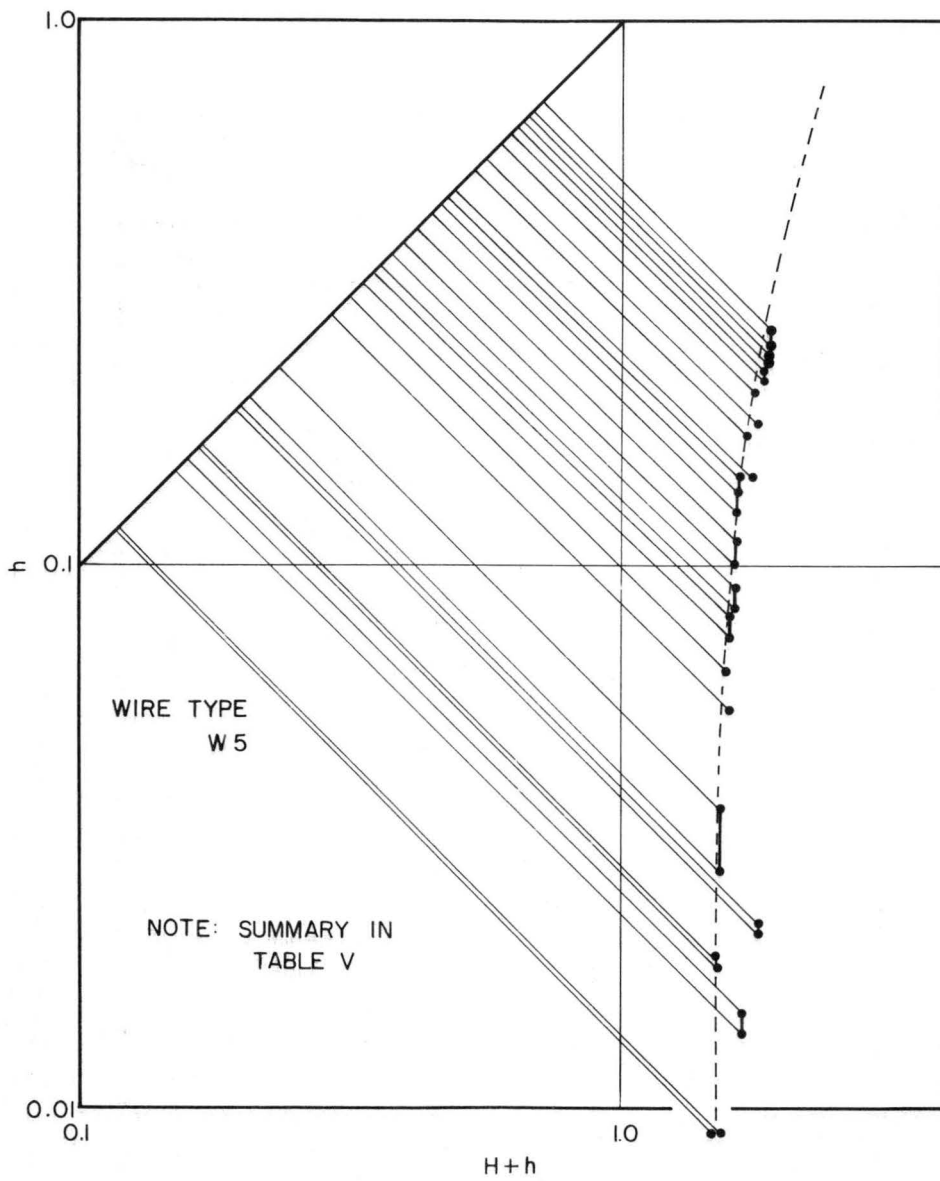


FIG. 25 SUSPENSION WIRE PROBE

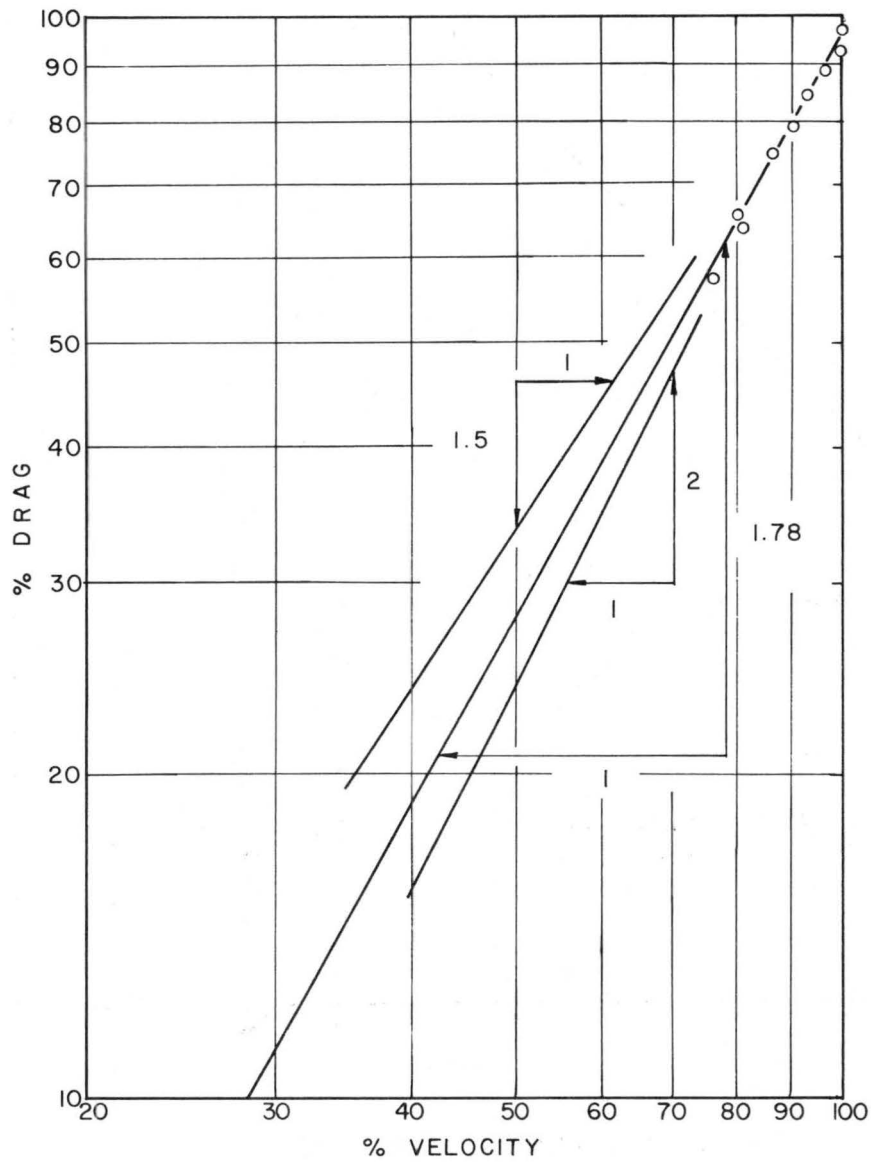


FIG. 26 FLUME TEST-SUSPENSION WIRE PROBE

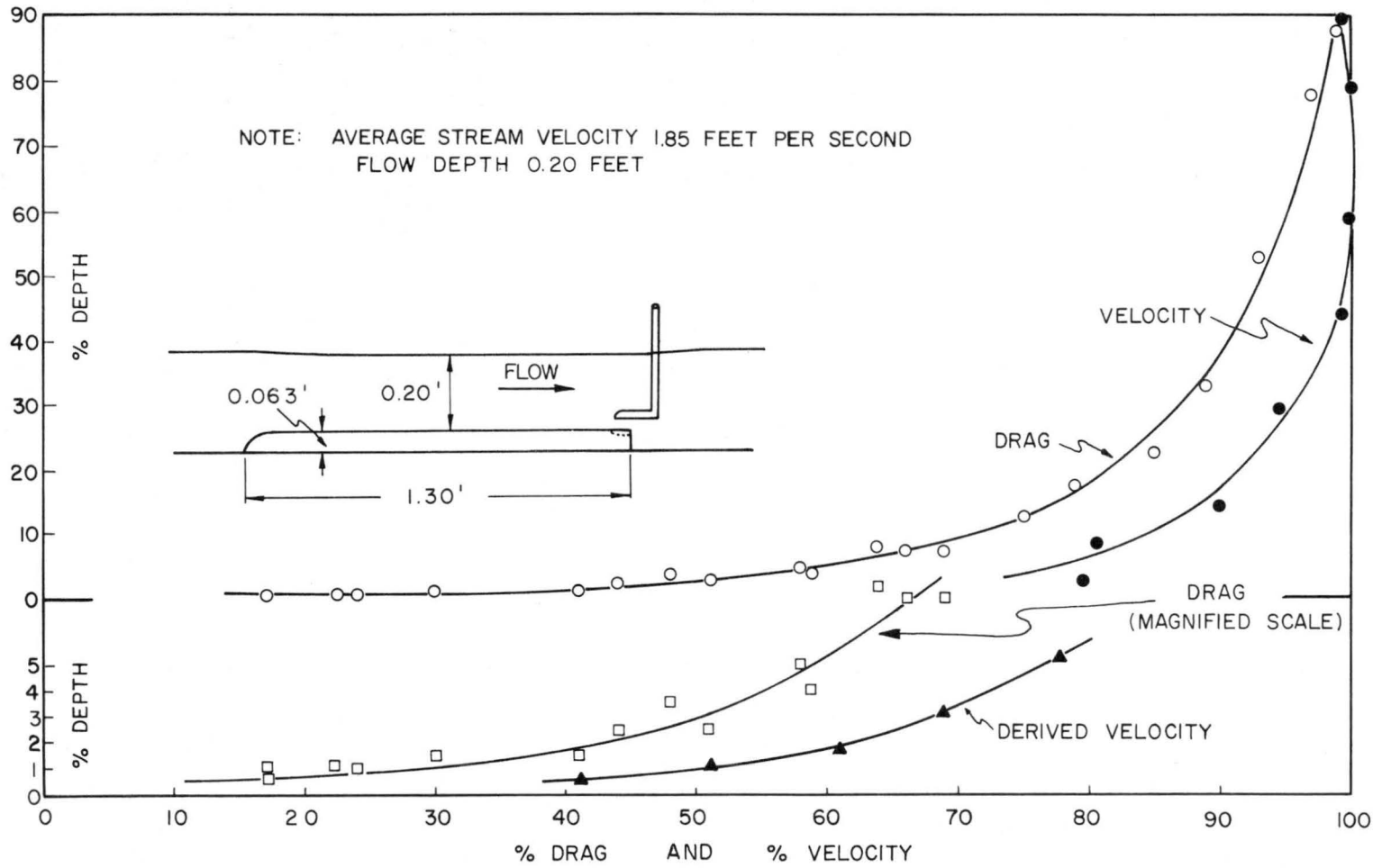


FIG. 27 SUSPENSION WIRE PROBE - 8 in WIDE FLUME

V. SUSPENSION WIRE PROBE - DYNAMIC RESPONSE

The suspension wire in its various applications thus far discussed, showed considerable sensitivity, in some cases to the detriment of steady average readings. It was a matter then of some interest to determine the dynamic response of the suspension wire probe in particular.

In a manner similar to that reported by Hsing Chuang (1962), the response of the probe to the vortex street generated by a fixed cylinder in the 8" flume was studied.

Again only a qualitative indication of the response was sought and the limited data obtained is included in Table VI, with the calculated dimensionless frequency parameter $F = \frac{fd^2}{\nu}$, where f is the frequency of the vortices, d the diameter of the fixed cylinder and ν the kinematic viscosity.

The results have been superimposed on the figure used by Chuang and presented in Fig. 28. The maximum frequency of vortices experienced was 66 c.p.s. as shown in Table VI. It was necessary in these tests to eliminate with a low pass filter network, the self-induced high frequency in the suspension wire itself. This frequency was of the order 1000 c.p.s. and depends on the wire length and the tension on the wire. It seems that this self-induced frequency could be readily controlled, in fact it was noted that it produced a particularly

TABLE VI
Suspension Wire Probe - Dynamic Response

d feet	f c.p.s.	$\nu \times 10^5$	$F = \frac{fd^2}{\nu}$	u f.p.s.	$R = \frac{ud}{\nu}$
0.0208	8.4	1.23	280	1.11	1870
	16.4		580	1.73	2930
	21.2		745	2.16	3660
	32		1130	3.30	5580
	40.5		1425	3.83	6460
	50.5		1.215	1800	4.90
0.0103	23.4	1.215	835	2.29	3920
	26.9		235	1.80	1530
	20.4		180	1.54	1300
	66		580	3.48	2950

stable signal which could be utilized in further applications of the instrument.

The qualitative results appear to agree quite well with the theoretical and experimental data included in Fig. 28 and considering that the suspension wire probe is integrating effects over a finite length it is felt that a study extended along these lines might be quite profitable.

VI SUSPENSION WIRE PROBE - RESPONSE TO SEDIMENT LOAD

The suspension wire responds to the effect of the drag of the fluid and provided the fluid is homogeneous, it is expected that a steady flow will produce a steady displacement of the wire satisfying the necessary equilibrium conditions.

Consider now the case of a non-homogeneous fluid such as water and entrained air or water and transported bed material.

It is interesting to speculate the response of the suspension wire subjected to such conditions. If a few random particles are present in the parent liquid and strike the wire a pulse is registered due to the momentum change of the particle becoming a force momentarily applied to the wire.

Equilibrium Equation (5) may be enlarged to allow for concentrated loads P_i and would then become:

$$-L(H+h) \tan \theta_A + \sum_i (x'_i - x) P_i = - \int_0^L (x' - L) p(x') dx' \quad (10)$$

The summation term is in effect a specific form of the integral term on the right side of Equation (10), see Karman and Biot (1940).

The interpretation of a series of random and intermittent loads would involve the difficulties of understanding the average flow and particle concentration relationships and methods for specifying the departures from the mean.

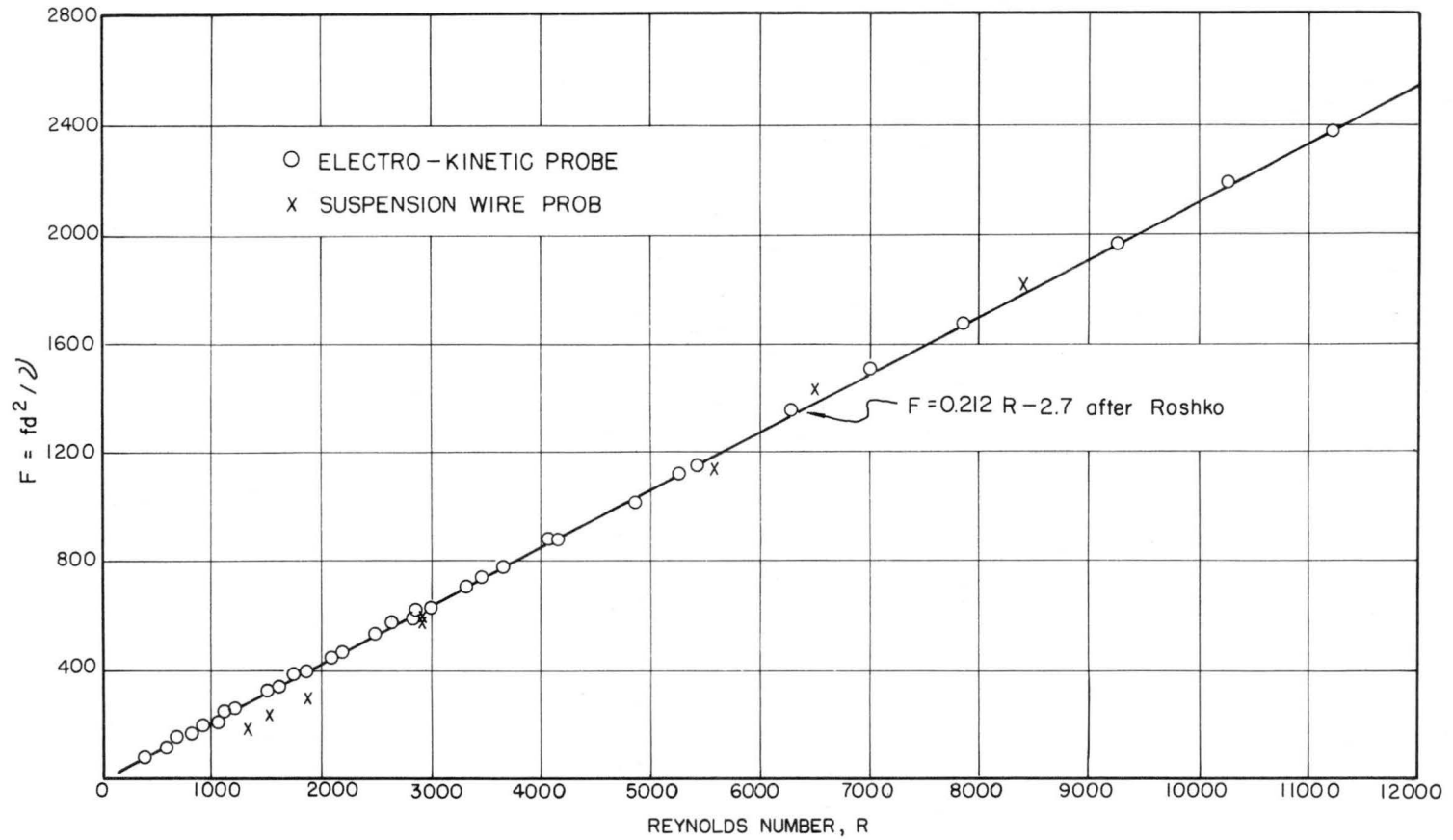
Suppose however that the concentration of the particles is increased to such an extent that the intermittent pulses then become almost continuous, then the average load exerted on the wire will be analogous to the behaviour of a homogeneous fluid.

Under these conditions the summation term in Equation (10) may be dispensed with and the right term viewed as the moment of the distributed load due to the particles impact.

The force on the wire is derived from the momentum of the particles and may be written according to H. Rouse (1947) in the form:

$$\Delta F = \Delta (\rho v Q) = \Delta (v \cdot \text{particle weight per sec}).$$

This equation can represent the particle momentum change in terms of the weight per second of the particles (or their concentration) and the velocity of the particles which will be slightly less than the stream velocity due to slip.



DIMENSIONLESS FREQUENCY PARAMETER VS. REYNOLDS NUMBER FOR A CIRCULAR CYLINDER

FIG. 28 SUSPENSION WIRE PROBE - DYNAMIC RESPONSE

A test was conducted in the 8" flume while separate studies of sediment load were being made. The material in use was size 1/8" Vestyron (ex - Germany) and the total load was approximately 85 grms per liter.

In Fig. 29 the drag readings and other data are included, showing two curves for the sediment drag effect - the result of two traverses.

Allowing for the velocity and drag ratios of the water alone (assumed distribution) the total reading

may be adjusted to exclude the effect of the water and the relative weight per second of sediment against depth deduced.

The above deductions are quite hypothetical as no real solution of the distribution was available to offer a comparison with these results.

It seems however that a heavy sediment load will behave as suggested above and more important, the suspension wire probe responded favorably under what might seem to be rather adverse conditions.

VII RECOMMENDATIONS

The report has been a summary of preliminary investigations of a suspension wire in a closed conduit and also in the form of a probe.

The number of tests and the accuracy of the readings were dictated by the main purpose of defining the operating principle and versatility of the device.

A number of practical problems, such as the physical characteristics of the wire were so immediately apparent, that the intention of developing the device for absolute measurement of the various quantities was postponed and only relative data submitted at this stage.

Although the response of the suspension wire has been examined for a number of interesting appli-

cations, one of the most significant possibilities that has not been specifically mentioned is that it may respond only to velocity effects and not pressure effects. This aspect might well fill a need for an instrument that is capable of observing transient velocities without being upset by the transient pressure field that is also present.

It is hoped that the problem of the choice of a suitable wire for a particular application can be solved quickly so that a careful study of accuracy and reliability can be made.

Tests with the output of the bridge recorded immediately on a roll chart are contemplated, thus utilizing the rapid response of the device and avoiding some loss of information that is otherwise inevitable.

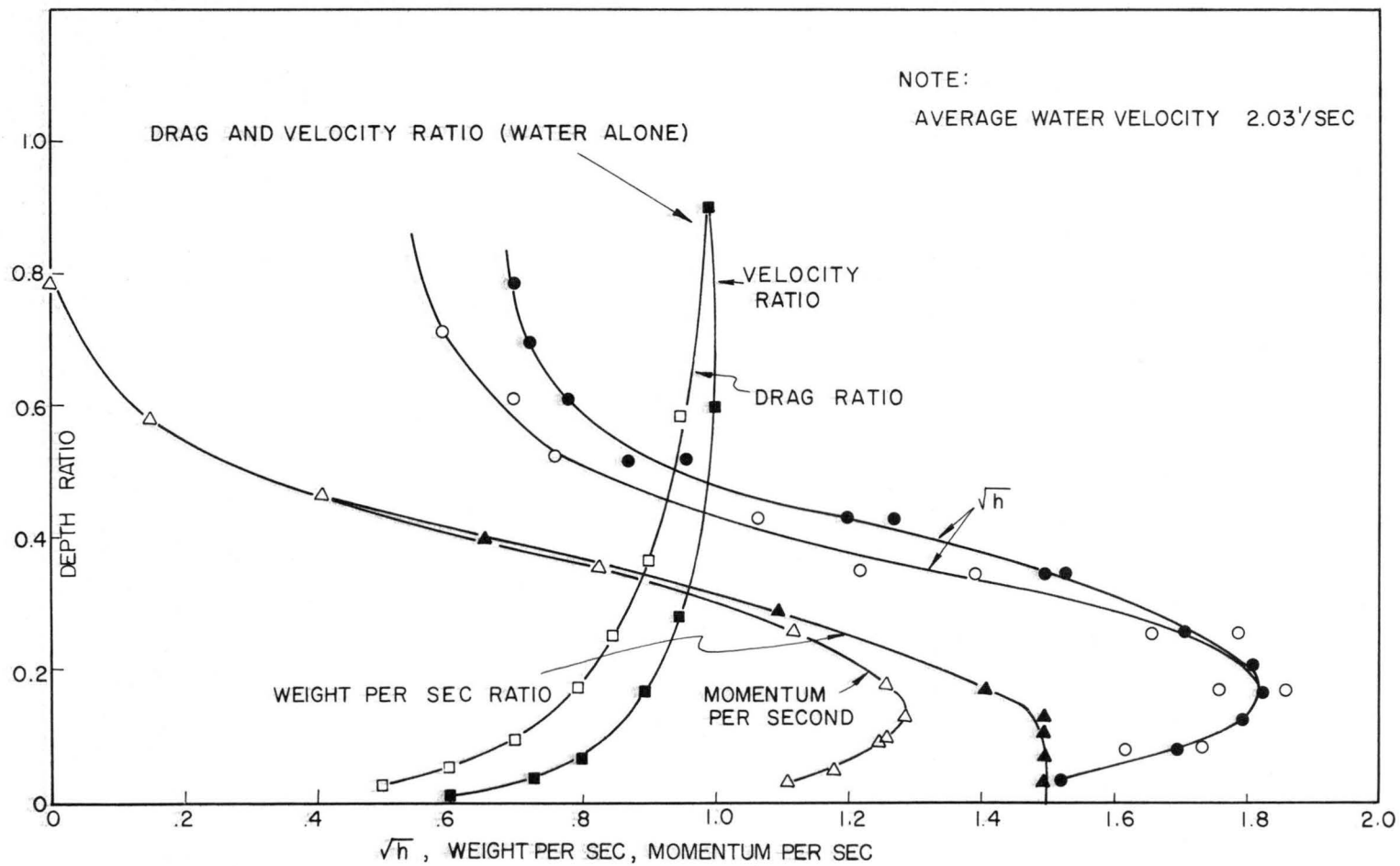


FIG. 29 SUSPENSION WIRE PROBE - RESPONSE TO SEDIMENT LOAD
(8" x 8" Tilting flume)

ACKNOWLEDGEMENTS

The assistance of the professional and technical staff of the Civil Engineering Department of Colorado State University is acknowledged, and especially the help and encouragement of A. R. Robinson and D. B. Simons.

REFERENCES

- Roshko, A. Jour. of Fluid Mechanics, Vol. 10, page 352, 1961.
- Steinman, D. B. Problems of Aerodynamic and Hydrodynamic Stability. Proc. Third Hydraulics Conf. Iowa, University of Iowa, Bulletin 31, page 136, 1946.
- Rouse, H. Seven Exploratory Studies in Hydraulics. Maximum amplitude of oscillation of a Cylinder due to its vortex wake, by Guyton, B. Le Tourneau B. W. and Player, R. C. Proc. of A.S.C.E. Journ. of Hydraulics, Vol. 84, HY4, Aug. 1956.
- Karmon, T. von, and Biot, M. A. Mathematical Methods in Engineering, McGraw Hill, 1940. Page 262, 282.
- Kay, J. M. An Introduction to Fluid Mechanics and Heat Transfer, Cambridge University Press, 1957. Page 183.
- Prandtl, L. and Tietjens, O. G. Applied Hydro- and Aeromechanics, Dover, 1957. Page 97.
- Rouse, H. Elementary Mechanics of Fluids, John Wiley, 1947. Page 111.